Reviewer #1:

Review of manuscript bg-2018-415 "On the role of climate modes in modulating the air-sea CO2 fluxes in Eastern Boundary Upwelling Systems by Riley X. Brady, Nicole S. Lovenduski, Michael A. Alexander, Michael Jacox, and Nicolas Gruber.

Summary:
This is a nice piece of work trying to link modes of natural climate variability to fluctuations of air-sea CO2 fluxes in Eastern Boundary Upwelling Systems (EBUS). The latter regions reveal strong upwelling of cold and nutrient-reach water masses, a prerequisite for ecological richness and diversity. Although small in area, EBUSs play an important role in the air-sea exchange of CO2. Utilizing 34 ensemble members of simulations with the Community Earth System Model (CESM-LENS) the authors have analyzed the correlations between natural climate variability (ENSO, PDO, NAO, ...) and air-sea CO2 fluxes for each of the four EBUSs.

The manuscript is clearly written and the conclusions comprehensible. Therefore, subject to very minor revisions I recommend publication in Biogeosciences.

We would like to thank referee #1 for their time in reviewing this paper. Their suggestions substantially improved this manuscript. Please see the revised manuscript with tracked changes at the bottom of this document.

Specific Comments:

1. page 5 equation 2: The variable U is not defined (presumably wind speed).

   Thank you for catching this error. We now define U as wind speed in page 5 line 10, since it is introduced as being a factor in calculating k.

2. page 5 last sentence: To compensate for autocorrelation ... This should be explained a bit more in detail. Readers not familiar with the statistical methodology will not understand it.

   Thank you for this suggestion. We agree that in its original form, the explanation was not entirely clear. We have now updated the manuscript to the following:

   > *Autocorrelation is prevalent in climate indices such as the NPGO and ENSO (Di Lorenzo and Ohman, 2013), and our annual smoothing further enhances autocorrelation in CalCS and CanCS air-sea CO_2 fluxes (see Sections 3.3.1 and 3.3.3). To compensate for this autocorrelation, we replace the t-statistic sample size N with an effective sample size N_{eff}, which quantifies the number of statistically independent measurements: ...*

3. page 6 lines 18+19: ... the data density of pCO2 in EBUS informing the SOM-FFN is on the order of the Southern Ocean, ... This statement is too vague. It would be good to be a bit more quantitative.

   Thank you for this suggestion. We have quantified this by taking the mean number of observations informing the SOM-FFN for each EBUS (following the regions shown

in Figure 2e and 2f) and for the Southern Ocean (south of 40S). Page 6 lines 18+19 were updated to the following:

Another important caveat is that the average number of pCO_2 observations in EBUS informing the SOM-FFN (637, 119, 517, and 195 for the CalCS, HumCS, CanCS, and BenCS, respectively) is on the order of the Southern Ocean (536), a notably undersampled region (Figure 2e and f; Bakker et al., 2016).

References

Bakker, D. C. E., Pfeil, B., OBrien, K. M., Currie, K. I., Jones, S. D., Landa, C. S., Lauvset, S. K., Metzl, N., Munro, D. R., Nakaoka, S.-I., Olsen, A., Pierrot, D., Saito, S., Smith, K., Sweeney, C., Takahashi, T., Wada, C., Wanninkhof, R., Alin, S. R., Becker, M., Bellerby, R. G. J., Borges, A. V., Boutin, J., Bozec, Y., Burger, E., Cai, W.-J., Castle, R. D., Cosca, C. E., DeGrandpre, M. D., Donnelly, M., Eischeid, G., Feely, R. A., Gkritzalis, T., González-Dávila, M., Goyet, C., Guillot, A., Hardman-Mountford, N. J., Hauck, J., Hoppema, M., Humphreys, M. P., Hunt, C. W., Ibánhez, J. S. P., Ichikawa, T., Ishii, M., Juranek, L. W., Kitidis, V., Körtzinger, A., Koffi, U. K., Kozyr, A., Kuwata, A., Lefèvre, N., Lo Monaco, C., Manke, A., Marrec, P., Mathis, J. T., Millero, F. J., Monacci, N., Monteiro, P. M. S., Murata, A., Newberger, T., Nojiri, Y., Nonaka, I., Omar, A. M., Ono, T., Padín, X. A., Rehder, G., Rutgersson, A., Sabine, C. L., Salisbury, J., Santana-Casiano, J. M., Sasano, D., Schuster, U., Sieger, R., Skjelvan, I., Steinhoff, T., Sullivan, K., Sutherland, S. C., Sutton, A., Tadokoro, K., Telszewski, M., Thomas, H., Tilbrook, B., van Heuven, S., Vandemark, D., Wallace, D. W., and Woosley, R. (2016). Surface Ocean CO2 Atlas (SOCAT) V4.

Di Lorenzo, E. and Ohman, M. D. (2013). A double-integration hypothesis to explain ocean ecosystem response to climate forcing. *Proceedings of the National Academy of Sciences*, 110(7):2496–2499.

Reviewer #2:

Summary:
I think this is a good paper that is publishable with minor to moderate revision. Some details of the methodology are insufficiently explained. The English is generally good, although there are some quirks of usage that suggest an inexperienced lead author whose more senior coauthors put rather less time into editing the text than they could have.

We would like to thank referee #2 for their careful review of this paper. Their suggestions substantially improved this manuscript. Please see the revised manuscript with tracked changes at the bottom of this document.

Overall structure:
I think that "Conclusions and Discussion" would be better entitled "Discussion and Conclusions", and Section 3 should be incorporated into the Results. The first paragraph of the Discussion covers a lot of different topics, and rehashes a lot of the Results. It would be better to lead off with a summation of the main points, and then further discussion of each, broken into a larger number of shorter paragraphs each focused on a specific topic.

Thank you for your suggestion. We have changed the final section to be called "Discussion and Conclusions." We have also incorporated Section 3 into the Results.

We have split the first paragraph of Section 5 into three smaller paragraphs covering separate topics (i.e., the seasonal cycle discussion, the general CO_2 flux response to modes of climate variability, and the more specific CO_2 flux response to climate variability.)

The Introduction meanders about a number of related topics in a way that could easily give the reader the impression that high-resolution regional hindcast simulations were employed (3/15-20). There is nothing wrong with mentioning the utility of such tools, but ideally one should try to structure the Introduction in a way that focuses on (1) what is the problem at hand? (2) what tools were used to address it? and (3) what is novel in the analysis that sets it apart from what is already in the literature?

Thank you for your suggestions. We have removed 3/15–20 and replaced it with a much briefer description of high-resolution simulations:

> *Regional hindcast simulations are beneficial for their higher spatial resolution and more accurate representation of a specific EBUS's dynamics, but they are limited to the analysis of a single EBUS, preventing a synchronous view across EBUS with a consistent modeling tool.*

Similarly, I dont think that the idea that previous EBC studies have not focused on CO2 (2/18, 3/8) is either accurate or relevant (and the sentence on 2/18-20 is simply ugly).

Thank you for your comments. We have edited 2/18–20 to read more cleanly:

> *So far, relatively few studies have truly assessed the longer-term variability of*

the air-sea CO_2 fluxes in EBUS, regardless of whether these variations are internal or forced.

Indeed, very few EBC studies have focused directly on the link between climate variability and air-sea CO_2 fluxes (Chavez et al., 1999; Friederich et al., 2002; Torres et al., 2003; Feely et al., 2006; Takahashi et al., 2003), in comparison to the response of physics and biology to climate variability (e.g., Chenillat et al., 2012; Chhak and Di Lorenzo, 2007; Di Lorenzo et al., 2008, 2009; Mantua et al., 1997; Cropper et al., 2014; Shannon et al., 1986; Reason et al., 2006; Hutchings et al., 2009; Chelton et al., 1982; Barber and Chavez, 1983; Barber and Chávez, 1986; Lynn and Bograd, 2002; Escribano et al., 2004; Frischknecht et al., 2015, 2017; Borges et al., 2003). We feel that mentioning this in 2/18 and 3/8 is useful to motivate the need for a study investigating air-sea CO_2 fluxes directly.

Statements like 7/27-29 are also unnecessary; this section is properly part of the Results, and statements like this belong in the Discussion (see also 6/11-13, 7/10-11).

Thank you for your suggestions. We excised 7/10–11 and 7/27–29 from the manuscript. We removed 6/11–13 and adapted 14/24–25 to read:

Due to model resolution, we do not resolve the coastal upwelling that induces vigorous outgassing within the first ∼50km of the coastline, such as in high resolution model solutions by Turi et al. (2014) and Fiechter et al. (2014).

Methods:
I dont think the definitions of the boundaries of the boxes are sufficiently explained. The outer boundaries of the boxes in Figure 3 are not parallel to the coastline, so "from the coastline to 800 km offshore" hardly seems adequate. Turi et al only use the 800 km figure in general terms, in reference to the approximate domain of influence of coastal upwelling on the thermocline depth. In Figure 1, the boxes seem to indicate an approximately (but not exactly) constant distance in the E-W direction. The boxes in Figure 3 are quite different. The regions considered in Figures 6-9 are similar, but not necessarily identical, to those in Figure 1. A clearer explanation is warranted, especially given that many of the analyses shown are for regional means over these boxes. (Note also that the second half of Section 2.2 has nothing to do with the topic specified in header.)

Thank you for your comments. Note that the boxes/boundaries used for statistical analysis are only showcased in Figure 1. Those shown in Figure 3 are just general boundaries (which span the full subplots of Figure 1) to point out that these regions exhibit significant unforced variability in CO_2 fluxes. The regions in Figures 6–9 are identical to those in Figure 1, but are just zoomed in a bit more on the region. We also point out in the caption of Figure 1 that these boundaries follow the model grid, i.e., that they are confined to 800km offshore zonally along the coarse grid.

We updated figure captions to clarify these points. To Figure 1, we added a note that the statistical boxes are confined to 800km "in the E–W direction." To Figure 3, we added "Here, the black boxes outline the general domain of the EBUS in this study but do not coincide with the statistical boundaries shown in Figure 1." Lastly, we renamed Section

2.2 to "Upwelling Regions and Anomalies" to account for the description of anomaly generation in the second half of that section.

For the regressions onto the climate indices, it should be be more clearly stated what the independent variable and its units are. References to a "1 degree El Nino" or 1 SD of NAO are better than nothing but not really adequate. If NINO3 is defined as a temperature anomaly in K, then a regression coefficient of CO2 flux on this index will have units of mol m-2 y-1 K-1 (e.g., 11/2). Similarly, the NAO has units of SLP. Im not sure what the units of the NPGO are. But a statement like "The direct regression of DeltaF onto the NPGO results in an anomalous uptake of 0.10 mol m-2 yr-1" seems incomplete, because the reader does not know how large an anomaly in the NPGO is required to give rise to X mol m-2 yr-1 of CO2 flux anomaly. The statement (12/10) that stronger winds in the CanCS "leads to the highest relative CO2 flux anomaly of any system" seems misleading because the independent variable for these regressions is different in each case. Maybe there is some basis for making this comparison, but it has not been clearly explained.

Thank you for this suggestion. We updated all cases where regression results were mentioned to account for the definition of the given mode of climate variability (K^{-1} for Nino3, σ^{-1} for NAO, NPGO, PDO). We have removed 12/10 per your suggestion.

The statistical tests applied are inadequately explained. The discussion of autocorrelation (5/27) appears out of nowhere without context. I agree that autocorrelation is important and you have to correct for it, but up to this point there has been no mention of statistical testing at all. First explain what test you are using to determine whether X is significantly different from 0, and state clearly what physical quantity X represents, then explain the effective sample size. The effective sample size is said to "replace the t-statistic sample size" (5/27), bu there is no mention of t-tests having been conducted; the only test specifically mentioned is the Mann-Kendall test (Table 1).

Thank you for your suggestion. We added the following description of our correlation/t-test methodology immediately following 5/26:

> *We use a Pearson product-moment correlation for all linear correlations performed in this study (e.g., between area-weighted CO_2 flux anomalies and climate indices for each EBUS). Our null hypothesis is that the two time series being compared are uncorrelated, following the Student's t-distribution with a significance level of $\alpha = 0.05$.*

We also further clarify the description of autocorrelation for the reader, replacing 5/27–28 with (see also response to Reviewer 1):

> *Autocorrelation is prevalent in climate indices such as the NPGO and ENSO (Di Lorenzo and Ohman, 2013), and our annual smoothing further enhances autocorrelation in CalCS and CanCS air-sea CO_2 fluxes (see Sections 3.3.1 and 3.3.3). To compensate for this autocorrelation, we replace the t-statistic sample size N with an effective sample size N_{eff}, which quantifies the number of statistically independent measurements: ...*

Lastly, we add a description of the Mann-Kendall test following 6/2:

> *We use a one-sided Mann-Kendall test to assess significance in trends (e.g., the long-term diffusion of anthropogenic CO_2 into EBUS). Our null hypothesis is that the trend is not significantly different from zero, with $\alpha = 0.05$.*

Model Evaluation:
I find parts of the discussion of model validation against SOM-FFN confusing. On the one hand, it is the best observational benchmark available, on the other hand, discrepancies are explained away as resulting from errors in the observational data product (6/17-21). I cant make sense of "CO2 fluxes in SOM-FFN are being informed by remote biogeochemical provinces more often than other regions of the ocean". I can guess at what is being stated here, but without a more specific explanation of what sort of bias it imparts to the data product, I dont think it helps to achieve the task at hand, which is to evaluate how physically realistic the model solution is.

We removed 6/19–21 ("CO_2 fluxes in SOM-FFN are being informed . . .) to avoid confusion for the reader.

Describing a model as biased without specifying the nature or sign of the bias (e.g., 6/15, 6/21) is not very useful. The beginning of 3.2 is misleading (CalCS shows very good results, HumCS much less so) and poorly worded. How about "CESM-LENS simulates the pCO2 seasonal cycle well for the Pacific EBUS, with larger error in the Atlantic regions"? (and change "Beginning with the CalCS" to simply "in the CalCS"). Again, this paragraph mixes up model evaluation, analyses of the model solution that do not have any analogue in the observations, and literature review. Again, I think this whole section should be included in the Results, and a clear separation of Results and Discussion attempted.

Thank you for your suggestion. 6/15 was changed to:

> *The CO_2 flux climatology in the Atlantic systems is more biased in the CESM-LENS, with a tendency for spurious or stronger outgassing than is suggested by the observational product.*

We feel that the statement immediately following 6/21 describes the nature of the bias, and it would be redundant to mention the outgassing bias in 6/21 directly. We changed the beginning of 3.2 per your suggestions:

> *CESM-LENS simulates the pCO_2 seasonal cycle well for the Pacific EBUS, with larger error in the Atlantic regions. In the CalCS, . . .*

Terminology:
"internal" variability in a model simulation is an analogue of "natural" climate variability

in the real world. I would prefer that the latter term be used except when the reference is specifically to climate model simulations. I find terms like "have some of the highest internally driven CO2 fluxes globally" very awkward. How about "have some of the highest unforced variability of CO2 flux of any part of the world ocean"?

Thank you for bringing this important point up. Our use of "internal" over "natural" was intentional in this manuscript. "Natural" variability encompasses both the internal/unforced contribution as well as natural external forcing from volcanic eruptions and the solar cycle. Although we agree that "unforced" is an appropriate alternative to "internal," the authors decided it was best to use "internal" for this study.

We have updated the abstract (1/7) to add (unforced) following internal. We have also updated the suggested sentence to "... highest unforced variability ..." for clarity.

Further, we have added a very careful description of "internal" and external (both natural and anthropogenic) forcing to the introduction, following 2/18:

> *Fundamentally, one can differentiate between variability arising from the processes that are purely internal to the climate system, and those that represent "external forcings", i.e., processes that impact the climate system from outside. The latter external processes can be further separated into natural and anthropogenic. The former includes variations induced by e.g., volcanic eruptions or changes in solar activity, while the latter includes changes in the concentration of greenhouse gases and other radiatively active constituents, or human-made changes in albedo. The internal variability can arise from within a subsystem itself (e.g., baroclinic instabilities leading to the formation of mesoscale eddies), or from the unforced interaction between components of the climate system.*

I think "values" is one of the most overused and abused words in scientific writing. Search out all occurrences and if possible replace with something specific. For example, on 10/8 one could replace "r-values" with "correlation coefficients" (see also 9/13-14, 11/22) and on 13/19 "mean values" could be "mean uptake". On 8/11, one cant even tell what physical quantity is being presented (it is the internal variability component of the standard deviation of the CO2 flux, but the reader has to go to the table caption to find this out).

Thank you for this suggestion. We replaced nearly every occurrence of "value(s)" with something more specific. We updated both the main text as well as figure labels and captions in Figs. 5–10.

There are many locations where "air-sea" could be added before "CO2 flux" in the interest of clarity (e.g., Figure 10 caption).

Thank you for this suggestion. We have added "air-sea" as a prefix to "CO_2 flux" in the Figure 10 and Table 1, 2 captions as well as in a few places throughout the text (2/18, 3/16, 3/34, 5/12, Sections 3.1 and 4.2, 8/3)

Some details:
1/21 "Upwelling delivers deep waters with respired nutrients to the surface, fueling primary production and ultimately supporting fisheries that are highly productive with respect to the small surface area they cover" Upwelling delivers waters rich in nutrients to the surface,

fueling primary production and ultimately supporting fisheries that are highly productive relative to the small surface area that they cover

Thank you. We have updated the manuscript to reflect your suggestion.

2/5 "contributing to the magnitude and determining the direction of air-sea CO2 fluxes" determining the sign and magnitude of the air-sea CO2 flux

Thank you. We have updated the manuscript to reflect your suggestion.

2/11 "more efficient biology" greater biological production

Thank you. We have updated the manuscript to reflect your suggestion.

2/21 delete "fractional"

Thank you. We have updated the manuscript to reflect your suggestion.

3/5 Is it accurate to refer to the NAO as a "decadal-scale oscillation"? I thought it was more like a white noise process with a very flat frequency spectrum.

Thank you for this clarification. We use the language "decadal-scale" based on section 2 of Hutchings et al. (2009). Note also that the original NAO paper (Hurrell, 1995) suggests that the NAO is a source of low-frequency variability that imparts "large decadal climate variations over the North Atlantic."

4/20-21 "In contrast ... CO2 fluxes." I would delete this entire sentence.

Thank you. We have removed this sentence from the manuscript per your suggestion.

7/13 "These dual peaks are driven by an interchanging importance between thermal and non-thermal effects." These two peaks are driven by an alternating dominance of thermal and non-thermal effects. (see also 12/15 and 12/18)

Thank you for your suggestion. We have edited 7/13 and 12/15 to reflect these changes.

7/22 "the BenCS pCO2 seasonal cycle nearly 180 degrees out of phase" This actually true of CanCS as well, although the amplitude is significantly underestimated in the model.

Thank you for catching this. 7/19 has been modified to read "However, CESM-LENS simulates a damped seasonal cycle that is approximately 180 degrees out of phase for pCO_2 in the CanCS ..."

9/23 change "During a positive NPGO event" to "During the positive NPGO phase"? (and delete "of the system")

Thank you. We have updated the manuscript to reflect your suggestion.

9/24 add "transport" after "DIC"

Thank you. We have updated the manuscript to reflect your suggestion.

9/27 "Because the system-wide contributions of SST and sDIC to the anomalous flux nearly balance each other, minor contributions from wind, salinity, sAlk, and freshwater flux push the system in favor of anomalous uptake" I think this is an overinterpretation. It looks to me like the SST contribution is larger than the sDIC, and even if the 4 smaller terms cancelled each other out the net would still be negative.

Thank you for this comment. Note in Table 2 that the SST contribution is only slightly larger than the sDIC contribution (-0.12 mol m^{-2} yr^{-1} vs. 0.11 mol m^{-2} yr^{-1}). Accounting for ensemble spread, some individual ensemble members have sDIC contributions that slightly outweigh SST, so the minor terms are an important contribution toward causing uptake anomalies.

10/27 change "influencer" to "influence"

Thank you. We have updated the manuscript to reflect your suggestion.

11/4 change "are in opposition to one another" to "are of opposite sign"

Thank you. We have updated the manuscript to reflect your suggestion.

11/14 change "advected warm waters from the equatorial Pacific" to "warm water advected from the equatorial Pacific"

Thank you. We have updated the manuscript to reflect your suggestion.

11/17 change "intensification of wind magnitude" to "increase in wind speed"

Thank you. We have updated the manuscript to reflect your suggestion.

11/23 "This encircles the climatological position of the Azores High, the atmospheric subtropical gyre which forces the CanCS." I have never heard the Azores High referred to as an "atmospheric subtropical gyre", although it is a large-scale anticyclone. But I have never heard this terminology before, and its generally bad practice to take existing terms and assign them new meanings without a compelling reason. I also dont think "encircles" is a good choice of words. How about "represents" (or "indicates" or "coincides with")?

Thank you for your suggestion. We agree that it is best to avoid assigning new labels. We've updated 11/23 to read "large-scale anticyclone" and have changed out "encircles" to "coincides with." We have also changed reference to "subtropical gyre" with "large-scale anticyclone" where appropriate (12/23)

11/32 "the linear Taylor approximation aligns exactly with the direct regression" I cant tell what this means.

Thank you for bringing this up. We have excised this statement to avoid confusion for the

reader.

11/33 "The NAO describes modifications to the intensity of atmospheric gyre circulation between the Azores High and Icelandic Low" The NAO represents fluctuations in the intensity of atmospheric circulation between the Azores High and Icelandic Low

Thank you. We have updated the manuscript to reflect your suggestion.

12/21 change "when sDIC and SST are of equal magnitude" to "when the sDIC and SST associated terms are of about equal magnitude"

Thank you. We have updated the manuscript to reflect your suggestion.

12/27-30 "The major EBUS ... variability in CO2 fluxes." another truly awful sentence: rewrite or delete

Thank you for your suggestion. We've excised this sentence as well as the sentences that follow it (12/27–33)

13/13 change "diffusion" to "mixing"

Thank you. We have updated the manuscript to reflect your suggestion.

13/7 delete "to" before "roughly"

Thank you. We have updated the manuscript to reflect your suggestion.

13/25 I think this statement requires a data or literature reference.

Thank you for this suggestion. For clarification, our comments on changes to the CO_2 flux seasonal cycle were based on our analysis of the CESM-LENS. We have added statements to this line clarifying that these are results from CESM-LENS to avoid confusion for the reader.

13/34 "the relative contributions of variables to anomalous CO2 fluxes" the relative contributions of different physical processes to anomalous CO2 fluxes

Thank you. We have updated the manuscript to reflect your suggestion.

14/4 "While not observed in our historical modeling study, modifications to modes of climate variability associated with the major EBUS could directly influence the magnitude of internally generated anomalies in CO2 fluxes in the future." I dont see how we know this. Such trends might exist in the ensemble data even if no one has yet attempted to detect them.

Thank you for your suggestion. We edited the text to be more clear, following 14/1–4 with: "These modifications to modes of climate variability suggested by the literature could directly impact the response of EBUS CO_2 flux anomalies to internal variability, thus affecting the conclusions of our study."

14/9 "we only present the leading mode of climate variability" Similarly, this may be true but I dont think it is demonstrated by the data shown in this paper. The authors simply focus, in each region, on what they EXPECT to be the most important mode; they dont actually test whether this is true.

Thank you for noticing this. We modified the manuscript to read: "We present the mode of climate variability that has the largest influence on CO_2 flux ..."

14/10-12 "we explain", "we were able to explain" not an appropriate use of first person (I suggest that the wording of all discussions of explained variance in this paragraph be reviewed.)

Thank you for your suggestion. We updated the manuscript to read "we account for" in both cases.

14/19 change "a coarse single model ensemble" to "a single coarse-resolution model"

Thank you. We have updated the manuscript to reflect your suggestion.

14/24 "do not directly resolve the coastal upwelling process which induces vigorous outgassing within the first O(10km) of the coastline" do not resolve the coastal up- welling that induces vigorous outgassing within the first ∼10 km of the coast.

Thank you. We have updated the manuscript to reflect your suggestion. Note that we used ∼50km which is a more accurate depiction of the length scale of outgassing if one is not to use O().

14/28-29 I agree with this sentiment, but you have to get the boundary conditions for the downscaling model from global models. So if those models have huge biases in the positions of major transition zones, its not clear that having resolution within a regional domain is going to do any good. This is a problem in the northwest Atlantic as well, as coarse resolution models have large and persistent biases in the location of the Gulf Stream separation from the coast.

Thank you for your comments. We agree that one requires boundary conditions from global models to downscale to higher resolution. However, Machu et al. (2015) show significant improvement in the physics and biogeochemistry of the Benguela Current through dynamical downscaling (i.e., even when inheriting biases through the coarse boundary conditions). Further, other techniques can help to ensure that the high resolution regional model has less bias than the coarse global model. For instance, Small et al. (2015) reduce the Benguela warm bias by also increasing atmospheric resolution and adjusting alongshore wind stress curl to be more realistic for the system. (Manuscript unchanged in response to comment)

Figure 5 contains a great deal of information, and the caption could be a bit clearer. Violin plots may not be familiar to some readers, and exactly what is shown in the right hand panels could be spelled out. Similarly, the caption to Table 2 could contain a great deal more detail.

Thank you for your suggestion. The following has been added to the end of Figure 5's caption:

> *The interior of the violin plot displays a box plot with the ensemble mean denoted as a white dot. Shading around the box plot reflects the ensemble distribution of correlations, which are mirrored on either side.*

The caption for Table 2 was updated to:

> *Estimated contributions of individual terms to air-sea CO_2 flux anomalies, ΔF, in response to a mode of climate variability using Equation 4. Each row under the Individual Terms header depicts the ensemble mean contribution and ensemble spread for Figures 6–9. The column "CalCS–PDOn" reflects results from the nearshore box in the CalCS in Figure 7, and "CalCS–PDOo" the offshore box. Σ is the sum of all contributing first-order terms (i.e., all rows under Individual Terms or the right hand side of Equation 4). ΔF is the direct regression of CO_2 flux anomalies onto the specified mode of climate variability (i.e., the left hand side of Equation 4).*

We also included units in Table 2 and Table 3 to reflect that these are responses to 1 unit of the given mode of climate variability (e.g., mol m^{-2} yr^{-1} σ^{-1})

References

Barber, R. T. and Chavez, F. P. (1983). Biological consequences of El Niño. *Science*, 222(4629):1203–1210.

Barber, R. T. and Chávez, F. P. (1986). Ocean variability in relation to living resources during the 1982–83 El Niño. *Nature*, 319:279 EP –.

Borges, M. F., Santos, A. M. P., Crato, N., Mendes, H., and Mota, B. (2003). Sardine regime shifts off Portugal: a time series analysis of catches and wind conditions. *Scientia Marina*, 67(S1):235–244.

Chavez, F., Strutton, P., Friederich, G., Feely, R., Feldman, G., Foley, D., and McPhaden, M. (1999). Biological and chemical response of the equatorial Pacific Ocean to the 1997-98 El Niño. *Science*, 286(5447):2126–2131.

Chavez, F. P., Pennington, J. T., Castro, C. G., Ryan, J. P., Michisaki, R. P., Schlining, B., Walz, P., Buck, K. R., McFadyen, A., and Collins, C. A. (2002). Biological and chemical consequences of the 1997–1998 El Niño in central california waters. *Progress in Oceanography*, 54(1):205–232.

Chelton, D. B., Bernal, P. A., and McGowan, J. A. (1982). Large-scale interannual physical and biological interaction in the California Current. *Journal of Marine Research*, 40(4):1095–1125.

Chenillat, F., Rivière, P., Capet, X., Di Lorenzo, E., and Blanke, B. (2012). North Pacific Gyre Oscillation modulates seasonal timing and ecosystem functioning in the California Current upwelling system. *Geophysical Research Letters*, 39(1).

Chhak, K. and Di Lorenzo, E. (2007). Decadal variations in the California Current upwelling cells. *Geophysical Research Letters*, 34(14).

Cropper, T. E., Hanna, E., and Bigg, G. R. (2014). Spatial and temporal seasonal trends in coastal upwelling off Northwest Africa, 1981–2012. *Deep Sea Research Part I: Oceanographic Research Papers*, 86:94–111.

Di Lorenzo, E., Fiechter, J., Schneider, N., Bracco, A., Miller, A. J., Franks, P. J. S., Bograd, S. J., Moore, A. M., Thomas, A. C., Crawford, W., Peña, A., and Hermann, A. J. (2009). Nutrient and salinity decadal variations in the central and eastern North Pacific. *Geophysical Research Letters*, 36(14).

Di Lorenzo, E. and Ohman, M. D. (2013). A double-integration hypothesis to explain ocean ecosystem response to climate forcing. *Proceedings of the National Academy of Sciences*, 110(7):2496–2499.

Di Lorenzo, E., Schneider, N., Cobb, K. M., Franks, P. J. S., Chhak, K., Miller, A. J., McWilliams, J. C., Bograd, S. J., Arango, H., Curchitser, E., Powell, T. M., and Rivière, P. (2008). North Pacific Gyre Oscillation links ocean climate and ecosystem change. *Geophysical Research Letters*, 35(8).

Escribano, R., Daneri, G., Farías, L., Gallardo, V. A., González, H. E., Gutiérrez, D., Lange, C. B., Morales, C. E., Pizarro, O., Ulloa, O., and Braun, M. (2004). Biological and chemical consequences of the 1997–1998 El Niño in the Chilean coastal upwelling system: a synthesis. *Deep Sea Research Part II: Topical Studies in Oceanography*, 51(20):2389–2411.

Feely, R., Takahashi, T., Wanninkhof, R., McPhaden, M., Cosca, C., Sutherland, S., and Carr, M.-E. (2006). Decadal variability of the air-sea co2 fluxes in the equatorial pacific ocean. *Journal of Geophysical Research: Oceans*, 111(C8).

Fiechter, J., Curchitser, E. N., Edwards, C. A., Chai, F., Goebel, N. L., and Chavez, F. P. (2014). Air-sea CO2 fluxes in the California Current: Impacts of model resolution and coastal topography. *Global Biogeochemical Cycles*, 28(4):371–385.

Friederich, G. E., Walz, P. M., Burczynski, M. G., and Chavez, F. P. (2002). Inorganic carbon in the central California upwelling system during the 1997–1999 El Niño–La Niña event. *Progress in Oceanography*, 54(1):185–203.

Frischknecht, M., Münnich, M., and Gruber, N. (2015). Remote versus local influence of ENSO on the California Current System. *Journal of Geophysical Research: Oceans*, 120(2):1353–1374.

Frischknecht, M., Münnich, M., and Gruber, N. (2017). Local atmospheric forcing driving an unexpected California Current System response during the 2015–2016 El Niño. *Geophysical Research Letters*, 44(1):304–311.

Hurrell, J. W. (1995). Decadal trends in the north atlantic oscillation: regional temperatures and precipitation. *Science*, 269(5224):676–679.

Hutchings, L., Van der Lingen, C., Shannon, L., Crawford, R., Verheye, H., Bartholomae, C., Van der Plas, A., Louw, D., Kreiner, A., Ostrowski, M., et al. (2009). The Benguela Current: An ecosystem of four components. *Progress in Oceanography*, 83(1-4):15–32.

Lynn, R. and Bograd, S. (2002). Dynamic evolution of the 1997–1999 El Niño–La Niña cycle in the southern California Current System. *Progress in Oceanography*, 54(1-4):59–75.

Machu, E., Goubanova, K., Le Vu, B., Gutknecht, E., and Garçon, V. (2015). Downscaling biogeochemistry in the benguela eastern boundary current. *Ocean Modelling*, 90:57–71.

Mantua, N. J., Hare, S. R., Zhang, Y., Wallace, J. M., and Francis, R. C. (1997). A Pacific Interdecadal Climate Oscillation with impacts on salmon production. *Bulletin of the American Meteorological Society*, 78(6):1069–1079.

Pauly, D. and Christensen, V. (1995). Primary production required to sustain global fisheries. *Nature*, 374(6519):255–257.

Reason, C., Florenchie, P., Rouault, M., and Veitch, J. (2006). Influences of large scale climate modes and Agulhas system variability on the BCLME region. In *Large Marine Ecosystems*, volume 14, pages 223–238. Elsevier.

Shannon, L. V., Boyd, A. J., Brundrit, G. B., and Taunton-Clark, J. (1986). On the existence of an El Niño-type phenomenon in the Benguela System. *Journal of Marine Research*, 44(3):495–520.

Small, R. J., Curchitser, E., Hedstrom, K., Kauffman, B., and Large, W. G. (2015). The Benguela upwelling system: Quantifying the sensitivity to resolution and coastal wind representation in a global climate model. *Journal of Climate*, 28(23):9409–9432.

Takahashi, T., Sutherland, S. C., Feely, R. A., and Cosca, C. E. (2003). Decadal variation of the surface water pco2 in the western and central equatorial pacific. *Science*, 302(5646):852–856.

Torres, R., Turner, D. R., Rutllant, J., and Lefèvre, N. (2003). Continued CO2 outgassing in an upwelling area off northern Chile during the development phase of El Niño 1997–1998 (July 1997). *Journal of Geophysical Research: Oceans*, 108(C10).

Turi, G., Lachkar, Z., and Gruber, N. (2014). Spatiotemporal variability and drivers of pCO2 and air–sea CO2 fluxes in the California Current System: an eddy-resolving modeling study. *Biogeosciences*, 11(3):671–690.

On the role of climate modes in modulating the air-sea CO_2 fluxes in Eastern Boundary Upwelling Systems

Riley X. Brady[1], Nicole S. Lovenduski[1], Michael A. Alexander[2], Michael Jacox[2,3], and Nicolas Gruber[4]

[1]Department of Atmospheric and Oceanic Sciences and Institute of Arctic and Alpine Research, University of Colorado, Boulder, CO, USA
[2]NOAA/ESRL, Boulder, CO, USA
[3]NOAA/SWFSC, Monterey, CA, USA
[4]Environmental Physics, Institute of Biogeochemistry and Pollutant Dynamics, ETH Zürich, Zürich, Switzerland

Correspondence: Riley X. Brady (riley.brady@colorado.edu)

Abstract. The air-sea CO_2 fluxes in Eastern Boundary Upwelling Systems (EBUS) vary strongly in time and space with some of the highest flux densities globally. The processes controlling this variability have not yet been investigated consistently across all four major EBUS, i.e., the California (CalCS), Humboldt (HumCS), Canary (CanCS), and Benguela (BenCS) Current Systems. In this study, we diagnose the ~~physical and biological mechanisms that contribute to historical (1920-2015)~~ climatic modes of the air-sea CO_2 flux variability in these regions between 1920-2015, using simulation results from the Community Earth System Model Large Ensemble (CESM-LENS), a global coupled climate model ensemble that is forced by historical and RCP8.5 radiative forcing. Differences between simulations can be attributed entirely to internal ~~climate variability~~(unforced) climate variability, whose contribution can be diagnosed by subtracting the ensemble mean from each simulation. We find that in the CalCS and CanCS, the ~~deviations from the ensemble mean, i.e., the~~ resulting anomalous CO_2 fluxes ~~, in the CalCS and CanCS~~ are strongly affected by large-scale extratropical modes of variability~~associated with atmospheric subtropical gyres:~~ , i.e., the North Pacific Gyre Oscillation (NPGO) and the North Atlantic Oscillation (NAO), respectively. The CalCS (CanCS) has anomalous uptake (outgassing) of CO_2 during the positive phase of the NPGO (NAO). ~~The~~ In contrast, the HumCS is mainly affected by El Niño Southern Oscillation (ENSO), with anomalous uptake of CO_2 during an El Niño event. Variations in dissolved inorganic carbon (DIC) and sea surface temperature (SST) are the major contributors to these anomalous CO_2 fluxes, and are generally driven by changes to large-scale gyre circulation, upwelling, the mixed layer depth, and biological processes. A better understanding of the sensitivity of EBUS CO_2 fluxes to modes of climate variability ~~may~~ are key to improve our ability to predict the ~~ocean–atmosphere carbon cycle in EBUS, which are particularly susceptible to ocean acidification~~future evolution of the atmospheric CO_2 source/sink characteristics of the four EBUS.

1 Introduction

The four major Eastern Boundary Upwelling Systems (EBUS) occur at the eastern edges of subtropical gyres in the Atlantic and Pacific oceans – the California (CalCS), Humboldt (HumCS), Canary (CanCS), and Benguela (BenCS) Current Systems. These regions are characterized by seasonal or permanent equatorward winds that cause upwelling due to both offshore Ekman

transport as well as wind stress curl-driven Ekman suction within the first 200 km of the coastline (Chavez and Messié, 2009). Upwelling delivers ~~deep waters with respired~~ waters rich in nutrients to the surface, fueling primary production and ultimately supporting fisheries that are highly productive ~~with respect~~ relative to the small surface area they cover (Ryther, 1969). Upwelled waters also have ~~an elevated~~ a high dissolved inorganic carbon (DIC) content, which ~~enhances the~~ causes initially at the surface an elevated partial pressure of carbon dioxide (pCO_2)~~and reduces the pH and~~ , a low pH, and a low carbonate ion concentration~~. The carbonate chemistry of EBUS is controlled by a complex interplay of physical and biological processes :~~ , i.e., a low saturation state with regard to $CaCO_3$ minerals. The high productivity fueled by the upwelling pushes the surface ocean pCO_2 quickly down again, and also raises the pH and the carbonate ion concentration again (Turi et al., 2014). Further processes including entrainment of subsurface waters, horizontal advection ~~, upwelling and~~ and mixing, vertical mixing, temperature changes, ~~photosynthesis,~~ respiration, and calcium carbonate formation and dissolution (DeGrandpre et al., 1998; King et al., 2007) ~~.~~ affect the surface pCO_2. Thus, the resulting pCO_2 distribution is the result of a complex interplay of physical and biological processes. These terms combine to dictate oceanic pCO_2, which drives the pCO_2 gradient between the ocean and atmosphere (ΔpCO_2), thus ~~contributing to the magnitude and determining the direction of~~ determining the sign and magnitude of the air-sea CO_2 ~~fluxes~~flux.

Although coastal oceans around the world have a small net contribution to the global air-sea CO_2 flux, they are characterized by a high CO_2 flux density, or magnitude of air-sea CO_2 exchange per unit area (Laruelle et al., 2010, 2014; Gruber, 2015; Laruelle et al., 2017). Low-latitude upwelling systems, such as the HumCS and CanCS, tend to be net outgassing systems, due to their relatively warm waters and persistent upwelling, which are not fully compensated for by enhanced biological productivity. Because of their colder temperatures and ~~more efficient biology~~greater biological production, mid-latitude systems, such as the CalCS and BenCS, act as weak CO_2 sinks that can become CO_2 sources during certain seasons (Borges and Frankignoulle, 2002; Hales et al., 2005; Cai et al., 2006; Gregor and Monteiro, 2013). Surface ocean pCO_2 and thus air-sea CO_2 flux in EBUS exhibits high temporal variability at sub-seasonal, seasonal, and interannual time scales (Friederich et al., 2002; González-Dávila et al., 2009; Leinweber et al., 2009; Evans et al., 2011; Turi et al., 2014)~~. While the pronounced temporal variability of CO_2 fluxes in EBUS has been documented by numerous studies, little work has been done to associate it directly with internal climate variability (variability arising from unforced interactions between components of the climate system).~~

~~As coastal systems provide the majority of marine resources harvested by humans (Pauly and Christensen, 1995) and CO_2 fluxes are notoriously difficult to measure, studies have instead focused on associating major modes of climate variability with variability in~~ , driven by different sets of processes: Fundamentally, one can differentiate between variability arising from the ~~physics and biology of EBUS (e.g., Barber and Chavez, 1983; Chavez et al., 2002). However, internal variability in EBUS CO_2 fluxes is important to study, as it imposes variability on the fractional uptake of anthropogenic carbon by the ocean as well as modifies the surface ocean pH, potentially leading to intermittent ocean acidification events in the future (Kwiatkowski and Orr, 2018; Landschützer et al., 2018). Previous studies have tended to analyze the influence of internal climate variability on CO_2 fluxes for a single EBUSand a single climate event.~~ processes that are purely internal to the climate system, and those that represent "external forcings", i.e., processes that impact the climate system from outside. The latter external processes can be further separated into natural and anthropogenic. The former includes variations induced by e.g.,

volcanic eruptions or changes in solar activity, while the latter includes changes in the concentration of greenhouse gases and other radiatively active constituents, or human-made changes in albedo. The internal variability can arise from within a subsystem itself (e.g., baroclinic instabilities leading to the formation of mesoscale eddies), or from the unforced interaction between components of the climate system.

So far, relatively few studies have truly assessed the longer-term variability of the air-sea CO_2 fluxes in EBUS, regardless of whether these variations are internal or forced. Notable exceptions are Friederich et al. (2002) who analyzed the impact of the El Niño Southern Oscillation (ENSO) ~~has been observed to drive anomalous CO_2 flux in both the CalCS (Friederich et al., 2002) and HumCS (Chavez et al., 1999)~~in the CalCS and Chavez et al. (1999) who did the same for the HumCS. El Niño (La Niña) tends to cause uptake (outgassing) anomalies in these systems, primarily through modifications to the thermocline depth and upwelling rates of nutrient- and carbon-rich waters, which in turn alters biological activity. However, upwelling-favorable winds can persist during some El Niños in the HumCS (Huyer et al., 1987), leading to persistent or enhanced outgassing of CO_2 to the atmosphere (Torres et al., 2003). Longer-term fluctuations in the CalCS arise from Pacific Decadal Variability. Although studies have linked the Pacific Decadal Oscillation (PDO) and North Pacific Gyre Oscillation (NPGO) to low frequency changes in upwelling rates, nutrient fluxes, ocean acidification, and fisheries in the CalCS ~~(e.g., Chenillat et al., 2012; Chhak and Di Lorenzo, 2007; Di L~~ (e.g., Chenillat et al., 2012; Turi et al., 2016; Chhak and Di Lorenzo, 2007; Di Lorenzo et al., 2008; Mantua et al., 1997), no work has been done to directly investigate the effect of decadal variability on Pacific EBUS CO_2 fluxes in particular. However, studies have shown that a positive PDO intensifies the trade winds along the equatorial Pacific, leading to intensified upwelling and thus outgassing (Feely et al., 2006; Takahashi et al., 2003) and lower pH and saturation states (Turi et al., 2016). The response of HumCS CO_2 fluxes to the PDO might be similar. To the best of our knowledge, there have been no studies exploring CO_2 flux sensitivity to large modes of climate variability in the two Atlantic EBUS. However, Cropper et al. (2014) found that the North Atlantic Oscillation (NAO) plays a major role in modulating interannual variability of coastal upwelling in the CanCS and Borges et al. (2003) link the NAO to decadal variability in sardine catch. Variability in upwelling and biology in the BenCS has been linked to Benguela Niños (Shannon et al., 1986), ENSO teleconnections, and the Southern Annular Mode (Reason et al., 2006; Hutchings et al., 2009). However, decadal-scale oscillations like the NAO or PDO do not appear to be present in the South Atlantic (Hutchings et al., 2009). In summary, prior research has illuminated the large temporal variability of pCO_2 and CO_2 fluxes in EBUS and few have analyzed the impacts of single climate events on anomalous CO_2 fluxes in the CalCS and HumCS. Past studies tend to focus instead on linking internal climate variability to upwelling, nutrients, and fish catch. Our study aims to address this gap by identifying the major mode of climate variability associated with anomalous CO_2 fluxes in the major EBUS and by further investigating the dynamics that underpin these anomalies.

~~Previous studies have utilized observations (*e.g.*, Boyd et al., 1987; Friederich et al., 2002; Chavez et al., 2002; Santana-Casiano et al., 2~~ ~~and high-resolution hindcast simulations (Jacox et al., 2015; Frischknecht et al., 2015; Turi et al., 2017; Mogollón and Calil, 2017)~~ ~~to explore the relationship between~~ We are thus particularly interested in elucidating the role of internal climate variability and ~~EBUS biogeochemistry, such as dissolved oxygen, pH, nitrate supply, and primary production.~~ less on the forced (external) sources of variability.

Direct observation is of course the most desirable tool for understanding the real world, but it is not feasible for this study due to the sparsity of pCO_2 and air-sea CO_2 flux measurements and the relatively short length of observational time series. Regional hindcast simulations are beneficial for ~~two main reasons. First, they tend to have a higher resolution than the standard 1^o x 1^o resolution of global Earth System Models (ESMs) and thus explicitly resolve the coastal upwelling process. Second, the ocean model component is generally forced by an atmospheric reanalysis product so that the model more closely resembles reality than a freely coupled ESM. However~~their higher spatial resolution and more accurate representation of a specific EBUS's dynamics, but they are limited to the analysis of a single EBUS, preventing a synchronous view across EBUS with a consistent modeling tool. Further, single realizations (i.e., observational products and hindcast simulations) provide a limited sample size of internal variability and confound the impacts of external forcing ~~(e.g., land use change, fossil fuel emissions, volcanic eruptions)~~ with internal climate variability. The ~~former~~ limited sample size is problematic, because ~~ENSO events~~ internal stochastic noise causes ENSO events to evolve differently in the tropics (Capotondi et al., 2015)~~and~~ . Moreover, mid-latitude atmospheric noise can obscure the tropical-extratropical connections associated with climate modes such as ENSO, causing a diversity of responses in EBUS (Deser et al., 2017, 2018). The latter makes it difficult to isolate the internal ~~component of~~ variability in CO_2 fluxes from the seasonal cycle and ~~anthropogenic and~~ other external forcing. One solution to this problem is to use a single-model ensemble that is derived by introducing perturbations to the initial state of the climate system. This gives rise to a set of realizations with unique representations of internal climate variability and gives one access to many hundred ENSO events. By performing historical experiments with increasing atmospheric CO_2 rather than a long control simulation, we can account for variability in air-sea flux of both natural CO_2 (the component of ocean CO_2 in equilibrium with pre-industrial atmospheric CO_2) and anthropogenic CO_2.

In this study, we utilize output from the single-model Community Earth System Model "Large Ensemble" (CESM-LENS; Kay et al., 2015; Lovenduski et al., 2016) to identify major modes of climate variability that are associated with ~~anomalous~~ air-sea CO_2 fluxes in the major EBUS. ~~We expand on this by investigating the physical and biological drivers that underpin these anomalies. The single-model ensemble allows for an assessment of both the forced signal and the CO_2 flux response to internal climate variability. Since the simulations are forced with historical CO_2 emissions, each member accounts for variability in both natural and anthropogenic CO_2. Furthermore, the~~ To better identify these internal variability-driven fluxes, we subtract from each ensemble member the ensemble mean fluxes, as the latter represents essentially just the externally forced component. This results in what we refer to as the "anomalous" fluxes. The availability of 34 simulations allows us to find statistically robust relationships between these resulting anomalous CO_2 fluxes and internal climate variability. We expand on this by investigating the physical and biological drivers that underpin these air-sea CO_2 flux anomalies.

2 Methods

2.1 Model Configuration

We utilize monthly mean output from 34 members of the CESM-LENS (Kay et al., 2015; Lovenduski et al., 2016), which is derived from the Community Earth System Model, version 1, with the Community Atmosphere Model, version 5 (CESM1(CAM5);

Hurrell et al., 2013). Along with standard atmosphere, ocean, land, and sea ice components, the CESM-LENS simulations include land and ocean biogeochemistry. The ocean biogeochemical component of CESM1(CAM5) is the Biogeochemical Elemental Cycling (BEC) model, which has three phytoplankton functional groups and tracks the cycling of C, N, P, Fe, Si, and O in the ocean. Further information on the implementation of BEC in CESM1 can be found in Moore et al. (2013) and Lindsay et al. (2014). The ocean component is the Parallel Ocean Program, version 2 (Smith et al., 2010) and has a nominal 1^o horizontal resolution with vertical resolution of 10 m through the upper 250 m, thereby resolving the Ekman layer. Due to the coarse horizontal resolution, neither curl-driven nor coastal upwelling is directly resolved, but both are represented in the model. A more detailed discussion of coastal upwelling in the CESM-LENS for the CalCS in particular can be found in ~~(Brady et al., 2017)~~Brady et al. (2017).

The 34 ensemble members of CESM-LENS were generated using round-off level (order 10^{-14} K) ~~level~~ perturbations in the initial atmospheric temperature ~~.~~(Kay et al., 2015). This generates an ensemble of simulations that diverge solely due to the influence of internal variability. Each ensemble member was forced with ~~a~~ common external forcing: historical radiative forcing from 1920 to 2005 and RCP8.5 radiative forcing from 2006 to 2100. ~~In contrast to a pre-industrial control simulation, CESM-LENS includes the addition of anthropogenic carbon to air-sea CO_2 fluxes.~~ Anthropogenic CO_2 ~~is~~ was explicitly separated from natural CO_2 by computing air-sea CO_2 fluxes relative to a constant 284.7 ppm pre-industrial atmosphere and subtracting it from CO_2 fluxes responding to the evolving atmosphere under historical and RCP8.5 radiative forcing.

2.2 Upwelling Regions and Anomalies

Upwelling regions in each EBUS span approximately the 10^o latitude of most active upwelling as defined by Chavez and Messié (2009); we shifted the CanCS upwelling domain north by 9^o to capture the more intense upwelling off the Western Sahara in CESM1 (Table 1). Following Turi et al. (2014), the EBUS upwelling regions span from the coastline to 800 km offshore, tracking the model coastline. The black outlines in Figure 1e–h display these regions. The CESM-LENS ensemble mean incorporates the seasonal cycle and any long-term anthropogenic trends for a given variable. We therefore removed the ensemble mean from each simulation to create a time series of anomalies produced solely by internal climate variability. Note that for air-sea CO_2 flux, these anomalies represent internal variability in the contemporary ~~air-sea~~ flux of CO_2, or the combined variability of natural and anthropogenic CO_2.

2.3 Climate Indices

Throughout this paper, we regress anomaly time series of variables from each EBUS onto climate indices. Climate index time series were available for each ensemble member for ~~Nino3,~~ the PDO, NAO, Atlantic Multidecadal Oscillation (AMO), ENSO, and Atlantic Meridional Overturning Circulation (AMOC) through the Climate Variability Diagnostics Package (CVDP; Phillips et al., 2014). We computed the NPGO index for each simulation following Di Lorenzo and Mantua (2016)~~, and these~~ . These indices are available through the CESM-LENS project page ~~on the NPGO~~(NPGO). Note that the NAO, NPGO, and PDO indices referred to in this study are based on normalized principal component time series and are thus reported in standard deviation (σ) units.

2.4 ~~Statistical Analysis and~~ Model Equations and Statistical Analyses

Air-sea CO_2 fluxes in CESM are computed following the parameterization of Wanninkhof (2014):

$$F = k(U) \cdot K_0 \cdot (pCO_2^o - pCO_2^a), \tag{1}$$

where ~~k~~ k represents the gas transfer velocity (dependent on the wind speed (U) squared), K_0 the solubility of CO_2 in seawater, and pCO_2^o and pCO_2^a the partial pressures of CO_2 in the surface ocean and atmosphere, respectively.

We use a linear Taylor expansion to quantify the relative contribution of each variable to the overall air-sea CO_2 flux anomaly in response to ~~internally generated~~ unforced variability following Lovenduski et al. (2007) and Turi et al. (2014),

$$\Delta F = \frac{\partial F}{\partial U}\Delta U + \frac{\partial F}{\partial pCO_2^{oc}}\Delta pCO_2^{oc}, \tag{2}$$

where $\frac{\partial F}{\partial U}$ and $\frac{\partial F}{\partial pCO_2^{oc}}$ are determined from the model equations and mean values in each EBUS. Δ's represent the linear regression of the given variable's anomalies onto a climate index. ~~The contributions~~ In addition to the linearization of the response, which results in us neglecting potentially important cross-derivative terms, we neglected further several terms in Equation 2. In particular, we neglected the role of temperature and salinity for the solubility K_0 and the gas transfer velocity $k(U)$. This is justified since the impact of salinity is small and the temperature sensitivity of the product $k(U) \cdot K_0$ is very small, owing to a strong cancellation effect. Further we neglected the contribution of changes in atmospheric CO_2, pCO_2^a, primarily because these variations are at least 10 times smaller than those seen in surface ocean pCO_2^{oc}.

The contribution from ΔpCO_2^{oc} is further decomposed into the contribution of changes in DIC, Alk, SST, and salinity~~terms:~~

$$\Delta pCO_2^{oc} = \frac{\partial pCO_2^{oc}}{\partial DIC}\Delta DIC + \frac{\partial pCO_2^{oc}}{\partial Alk}\Delta Alk + \frac{\partial pCO_2^{oc}}{\partial T}\Delta T + \frac{\partial pCO_2^{oc}}{\partial S}\Delta S. \tag{3}$$

~~Because~~ The changes in DIC and Alk ~~can be diluted~~ induced by freshwater fluxes ~~, we introduce~~ have a strongly opposing influence on pCO_2, thus it is often more instructive to separate this effect on DIC and Alk from the others, and to summarize all salinity related terms into a freshwater term (see Lovenduski et al. (2007) for details). The remaining, non-salinity driven changes in DIC and Alk are referred to then as the salinity-normalized DIC (sDIC) and Alk (sAlk),

$$\Delta F = \frac{\partial F}{\partial U}\Delta U + \frac{S}{S_0}\frac{\partial F}{\partial DIC}\Delta sDIC + \frac{S}{S_0}\frac{\partial F}{\partial Alk}\Delta sAlk + \frac{\partial F}{\partial fw}\Delta fw + \frac{\partial F}{\partial T}\Delta T + \frac{\partial F}{\partial S}\Delta S. \tag{4}$$

Due to the significance of sDIC anomaly contributions to the total CO_2 flux anomaly in EBUS, we approximate the mechanisms controlling sDIC anomalies following Lovenduski et al. (2007),

$$\frac{d(sDIC')}{dt} = J'_{circ} + J'_{bio} + J'_{ex} \tag{5}$$

where J'_{circ}, J'_{bio}, and J'_{ex} represent the sources and sinks of sDIC′ from circulation, biology, and CO_2 flux anomalies integrated over the upper 100m, respectively. ~~See~~ We refer the reader to Lovenduski et al. (2007, their Equation 4) for additional details on these terms and their Appendix B for the computation of J'_{bio} in particular.

~~To compensate for autocorrelation that is characteristic of climate indices~~ We use a Pearson product-moment correlation for all linear correlations performed in this study (e.g., between area-weighted CO_2 flux anomalies and climate indices for each EBUS). Our null hypothesis is that the two time series being compared are uncorrelated, following the Student's *t*-distribution with a significance level of $\alpha = 0.05$.

Autocorrelation is prevalent in climate indices such as the NPGO and ENSO (Di Lorenzo and Ohman, 2013), and our annual smoothing further enhances autocorrelation in CalCS and CanCS air-sea CO_2 fluxes (see Sections 3.3.1 and ~~is also introduced from smoothing~~ 3.3.3). To compensate for this autocorrelation, we replace the *t*-statistic sample size *N* with an effective sample size ~~,~~ N_{eff}, which quantifies the number of statistically independent measurements:

$$N_{eff} = N\left(\frac{1 - r_1 r_2}{1 + r_1 r_2}\right) \tag{6}$$

where r_1 and r_2 are the lag-1 autocorrelation coefficients of the two time series being correlated (Bretherton et al., 1999; Lovenduski and Gruber, 2005). ~~N_{eff} represents the number of statistically independent measurements.~~

We use a one-sided Mann-Kendall test to assess significance in trends (e.g., the long-term diffusion of anthropogenic CO_2 into EBUS). Our null hypothesis is that the trend is not significantly different from zero, with $\alpha = 0.05$.

3 ~~Model Evaluation~~Results

3.1 Model Evaluation

CESM-LENS air-sea CO_2 flux climatologies and pCO_2 seasonal cycles were compared to the SOM-FFN (Self-Organizing Map-Feed Forward Network) product from Landschützer et al. (2017) along the four major EBUS outlined by Chavez and Messié (2009). The SOM-FFN is a CO_2 flux product based on numerous observational datasets and is made available at monthly resolution spanning 1982-2015 at 1^ox1^o global resolution. Extensive details on and validation of the procedure can be found in Landschützer et al. (2013) and Landschützer et al. (2016). The SOM-FFN does not include coastal estimates, which presumably would have stronger outgassing due to coastal and curl-driven upwelling of DIC-enriched waters. Another important caveat is that the average number of pCO_2 observations in EBUS informing the SOM-FFN (637, 119, 517, and 195 for the CalCS, HumCS, CanCS, and BenCS, respectively) is on the order of the Southern Ocean (536), a notably undersampled region (Figure 2e and f; Bakker et al., 2016). An extension of the SOM-FFN approach to the coastal ocean by Laruelle et al. (2017) demonstrated that the coastal pCO_2 values are not substantially different from the offshore, so that the conclusions drawn from the open ocean Landschützer product still hold.

3.2 ~~CO_2 Flux Climatology~~

3.1.1 Air-sea CO_2 Flux Climatology

The mean state of Pacific EBUS CO_2 fluxes is particularly well-modeled in CESM-LENS (Figure 1). The CESM-LENS captures the meridional gradient of poleward uptake and equatorward outgassing of CO_2 in the CalCS (Figure 1e). In ~~this~~

and the other EBUS, the coarse resolution model is not capable of resolving the narrow band of nearshore CO_2 outgassing found in high resolution model solutions (e.g., Turi et al., 2014; Fiechter et al., 2014). In the the HumCS, the model depicts the strong outgassing that is characteristic of a tropical upwelling system (Figure 1f). The CO_2 flux climatology in the Atlantic systems is more biased in the CESM-LENS, with a tendency for spurious or stronger outgassing than is suggested by the observational product. While the SOM-FFN portrays a meridional gradient of relatively weak CO_2 fluxes in the CanCS, the CESM-LENS simulates strong outgassing along the Western Sahara (Figure 1c and g). However, note that the SOM-FFN does not include coastal estimates, which presumably would have stronger outgassing due to coastal and curl-driven upwelling of DIC-enriched waters. Another important caveat is that the data density of pCO_2 in EBUS informing the SOM-FFN is on the order of the Southern Ocean, a notably undersampled region (Figure 2e and f; Bakker et al., 2016). In turn, the EBUS CO_2 fluxes in SOM-FFN are being informed by remote biogeochemical provinces more often than other regions of the ocean (see Landschützer et al., 2014, their Figure 1). The BenCS has the most biased CO_2 flux climatology of the major EBUS in CESM-LENS. Although it simulates the proper meridional gradient, the ougassing cell is nearly 10^o too far south and is significantly stronger than in the SOM-FFN (Figure 1d and h).

The BenCS has larger physical biases in CESM-LENS than all other EBUS. Its SST bias is in excess of 7^oC with the nominal 1^o atmospheric resolution, compared to less than a 1^oC bias in the CalCS and CanCS, and a 1–3^oC bias in the HumCS (pers. comm. with RJ Small, 2018). Further, the BenCS only improves to a 5^oC bias at 0.5^o atmospheric resolution (Gent et al., 2010) . This bias is likely driven by the fact that the Angola-Benguela Front is simulated too far south, in addition to deficiencies in upwelling and meridional transport that are caused by unrealistic alongshore wind stress structure (Small et al., 2015). Because these deficiencies are specific to the BenCS, we will only discuss its representation of the pCO_2 seasonal cycle in Section 3.23.1.2, and its internal variability in CO_2 fluxes in Section 4.13.2, but will not perform a full analysis on its connections to larger-scale climate variability.

3.2 *p*CO_2 Seasonal Cycle

3.1.1 *p*CO_2 Seasonal Cycle

CESM-LENS simulates the pCO_2 seasonal cycle for the EBUS with similar accuracy to its depiction of the mean state – the Pacific systems are generally well-modeled, while larger biases exist well for the Pacific EBUS, with larger error in the Atlantic regions. Beginning with EBUS. In the CalCS, CESM-LENS nearly perfectly matches the SOM-FFN in both amplitude and phase (Figure 2a). The system exhibits its maximum pCO_2 (and thus CO_2 outgassing) in August, and its minimum pCO_2 (and thus CO_2 uptake) in April. We further decomposed the model seasonal cycle into its thermal component (driven by the seasonality of SST) and its non-thermal component (driven by the seasonality of factors such as DIC, ALK, and salinity) following Takahashi et al. (2002). This decomposition suggests that the phase of the CalCS seasonal cycle is determined by thermal (solubility) effects, with its amplitude modulated by non-thermal factors (Figure 2a). These non-thermal factors are almost entirely driven by the seasonal cycle of DIC (not shown), which is characterized by photosynthetic uptake of CO_2 in the summer and fall, coinciding with upwelling season. These dynamics are supported by the high-resolution modeling study of

~~Turi et al. (2014), their Figure 9a.~~ In the HumCS, both CESM-LENS and SOM-FFN suggest a dual peak in the seasonal cycle of pCO_2, although the model and observational product slightly disagree in phase and amplitude (Figure 2b). These ~~dual~~ two peaks are driven by an ~~interchanging importance between~~ alternating dominance of thermal and non-thermal effects. During the austral summer/fall, warm temperatures lead to enhanced pCO_2 that is slightly compensated for by increased biological activity, similar to the singular peak of the CalCS. In the austral winter/spring, intense upwelling of DIC-enriched waters and reduced biological activity that is slightly compensated for by cooler waters leads to a secondary pCO_2 peak (Kämpf and Chapman, 2016). The SOM-FFN suggests that the CanCS behaves similarly to the CalCS, with a single pCO_2 peak in late summer/fall that is in phase with the seasonal cycle of SST (Figure 2c). However, CESM-LENS simulates ~~an extremely~~ a damped seasonal cycle that is approximately 180 degrees out of phase for pCO_2 in the CanCS that results from a delicate balance between thermal and non-thermal effects of similar magnitudes. Despite the thermal and non-thermal effects being in the proper phase for a northern hemisphere system, the SST seasonal cycle is too weak and the DIC seasonal cycle too strong in the CanCS in CESM-LENS. Lastly, we find that CESM-LENS simulates the BenCS pCO_2 seasonal cycle nearly 180 degrees out of phase with the SOM-FFN representation (Figure 2d). Similar to the CanCS, the thermal and non-thermal effects are in the proper phase. However, there is a large bias in the magnitude of the DIC seasonal cycle, which overwhelms the thermal seasonality and drives the pCO_2 seasonal cycle entirely out of phase. ~~This bias in the pCO_2 seasonal cycle further illuminates deficiencies in CESM1 in simulating the BenCS. Note that for all the EBUS, the dominance of the thermal effects is likely due to the fact that our area-weighted region encompasses a large domain that is driven by gyre-scale dynamics and downwelling. We would expect non-thermal factors to play an important role in dictating pCO_2 seasonality nearshore in a high-resolution simulation, such as in Turi et al. (2014), their Figure 9b.~~

4 ~~Results~~

3.1 Internal Variability in Upwelling Systems

We emphasize the magnitude of internal variability in EBUS air-sea CO_2 fluxes in Figure 3 by showing the ensemble mean standard deviation of air-sea CO_2 flux anomalies (ensemble mean subtracted) at each location across the global ocean. Save for the Southern Ocean and subpolar Arctic, the EBUS emerge as regions of high internal variability on a global scale. The HumCS, CanCS, and BenCS in particular have some of the highest ~~internally driven~~ unforced variability in CO_2 fluxes globally. The CalCS has comparatively low internal variability in CO_2 fluxes. The EBUS generally have higher internal variability than other coastal regions and are particularly distinct from the major western boundary currents, which appear to be influenced very little by internal variability (Figure 3). The internal variability can also be isolated as one constituent of the area-weighted CO_2 flux time series for each of the four EBUS, the others being the forced trend and seasonal cycle (Figure 4 (a–d)). The largest absolute internal variability component of the standard deviation of CO_2 flux is found in the BenCS ~~and HumCS with values of (~~0.98 mol m^{-2} yr^{-1} ~~and)~~ and the HumCS (1.20 mol m^{-2} yr^{-1} ~~, respectively (;~~ Table 1). The BenCS is uniquely exposed to variability from the Southern Ocean and Agulhas Current (Reason et al., 2006). The HumCS likely has intense variability due

to its proximity to the tropical Pacific Ocean and thus rapid communication with ENSO (e.g., Colas et al., 2008; Montes et al., 2011).

All four systems have statistically significant trends toward a weaker CO_2 source or greater CO_2 sink over 1920–2015 due mainly to the invasion of anthropogenic carbon from the atmosphere (Figure 4; Table 1). Note that in the CanCS and BenCS, there is a trend toward more outgassing of natural CO_2, which is compensated for by the relatively large uptake tendency of anthropogenic CO_2 (Table 1). The long-term trend forces the HumCS, CanCS, and BenCS to act as intermittent seasonal sinks by 2015 in some realizations due to the combination of the long-term trend and internal variability (Figure 4). The BenCS and CanCS have the largest uptake of anthropogenic CO_2 over the historical period, although the HumCS has a relatively large uptake of both natural and anthropogenic CO_2 (Table 1). For the HumCS and BenCS, the contemporary CO_2 flux trend is on the order of the magnitude of their seasonal cycles over the course of 96 years. The CanCS is a unique case, where the contemporary trend is more than double the magnitude of its seasonal cycle (Table 1).

The magnitude of internal variability in the combined natural and anthropogenic CO_2 fluxes is greater than that of the seasonal cycle for the majority of systems. The non-seasonal component of the total variability (the sum of the seasonal and internal components) is 59% for the HumCS, 73% for the CanCS, and 56% for the BenCS (Table 1). Only the CalCS has a stronger seasonal cycle of CO_2 flux than internal variability, but the non-seasonal component still accounts for 33% of the total variability in this system (Table 1). ~~Perhaps for the CalCS, as well as the other EBUS, more significant internal variability would be captured at a higher resolution that resolves coastal upwelling, such as in Turi et al. (2014, their Figure 8c).~~ Lastly, internal variability in CO_2 fluxes tends to be phase-locked with the seasonal cycle, as the peak magnitudes of internal variability track the ridges and troughs of the seasonal component (Figure 4).

3.2 Climate Variability and Air-sea CO_2 Fluxes

Our primary goal for each EBUS was to identify the mode of climate variability most strongly associated with its CO_2 flux anomalies. We correlated area-weighted anomalies from the black boxes in Figure 1e–h for each simulation with every grid cell globally for a set of predictor variable anomalies: SST, sea level pressure (SLP), 10m wind speed, and wind stress curl. We then assessed the ensemble mean of the correlations to determine the mode of climate variability associated with the given global spatial pattern. Figure 5 displays one ensemble mean correlation case for the CalCS (a), HumCS (b), and CanCS (c) as well as violin plots showing the spread of correlations across the 34-member ensemble for Pacific (Figure 5d–e) and Atlantic (Figure 5f) modes of variability.

3.2.1 California Current

The correlation between CalCS CO_2 flux anomalies and SSTa yields a map suggestive of Pacific Decadal Variability, due to the zonal dipole of correlations in the North Pacific (Figure 5a; Mantua and Hare, 2002; Di Lorenzo et al., 2008). Although similar in structure to the PDO, this map most closely resembles the NPGO (Di Lorenzo et al., 2008). In fact, correlations between the model-based NPGO with annual smoothing and CalCS CO_2 flux yields ~~an r-value~~ a correlation coefficient of -0.49 $\pm$ 0.04. In

comparison, linear correlations with the PDO result in ~~an r-value~~ a correlation coefficient of 0.24 ± 0.05 (Figure 5d). Thus, we highlight the NPGO as the major mode of climate variability associated with anomalous CO_2 flux in the CalCS.

We find that the CalCS has a single-signed response to the NPGO with anomalous uptake of CO_2 during a positive event, intensifying the mean state of the system as an uptake site (Figure 6). The direct regression of ΔF onto the NPGO results in an anomalous uptake of 0.10 mol m^{-2} yr^{-1}~~(~~ σ^{-1} (where "σ" refers to one standard deviation of the normalized principal component time series for the NPGO; Table 2), which is roughly 24% of the long-term historical CO_2 flux mean of -0.42 mol m^{-2} yr^{-1}. The primary contributions to this uptake anomaly come from variations in SST and sDIC, which are mainly driven by changes to offshore gyre dynamics. As the oceanic expression of the North Pacific Oscillation, the NPGO is associated with intensified geostrophic circulation, resulting in increased transport in both the California and Alaskan Coastal Currents (Di Lorenzo et al., 2008). Further, a positive NPGO leads to enhanced upwelling-favorable winds south of Cape Mendocino (Figure S1). During ~~a positive NPGO event~~the positive NPGO phase, the entire CalCS cools, increasing the CO_2 solubility ~~of the system~~ (Figure 6, Figure S1). Although downwelling is enhanced offshore, increased DIC transport from the Alaskan Gyre leads to a tendency for outgassing of CO_2 (Figure S1). Nearshore south of Cape Mendocino, increased upwelling of DIC-enriched waters is compensated for by photosynthesis, leading to near-zero CO_2 flux anomalies (Figure S2). North of Cape Mendocino, weakened upwelling and low subsurface DIC anomalies lead to enhanced uptake anomalies (Figures S1, S2). Because the system-wide contributions of SST and sDIC to the anomalous flux nearly balance each other, minor contributions from wind, salinity, sAlk, and freshwater flux push the system in favor of anomalous uptake (Figure 6).

The CalCS has the largest relative ensemble spread in sDIC and sAlk (Figure 6; Table 2). This is potentially because of inter-simulation variability in the response of CalCS dynamics to the NPGO due to atmospheric noise (as in the case of ENSO in Deser et al., 2017, 2018) which can directly alter the biogeochemical properties of source waters that feed the region (Pozo Buil and Di Lorenzo, 2017). Although the linear Taylor expansion approximates a CO_2 flux anomaly nearly half that of the direct regression of ΔF onto the NPGO, it is still of the same sign. This discrepancy is due to the influence of higher-order and cross-derivative terms that we did not account for in our linear approximation.

We also performed this analysis for the CalCS response to a 1σ positive (warm) phase of the PDO (Figure 7a and b). Every ensemble member displayed a dipole response to the PDO (not shown), with anomalous uptake in the nearshore region south of Cape Mendocino, and anomalous outgassing elsewhere in the domain (Figure 7c). This was the only case in which we found a non single-signed response across all ensemble members to any mode of climate variability investigated. However, note that the dipole pattern is quite similar to that of the CalCS response to the NPGO (Figure 6b). Both the nearshore and offshore regions have modest correlations with the PDO, with ~~r-values~~ correlation coefficients of -0.16 ± 0.03 and 0.28 ± 0.05, respectively. The positive phase of the PDO results in anomalously warm SSTs along the CalCS and causes weaker and shallower upwelling cells with higher retention of nutrient- and carbon-depleted surface waters (Figure S3; Chhak and Di Lorenzo, 2007). This aligns with the inverted contributions of SST and sDIC in Figure 7a and b relative to the contributions of these terms in response to the NPGO (Figure 6a). The warming of CalCS SSTs during a positive phase of PDO causes a reduction of CO_2 solubility and thus a tendency toward outgassing (Figure 7). Anomalous poleward coastal winds associated with the positive phase of the PDO result in reduced coastal and curl-driven upwelling along the entire coastline, and weakened curl-driven downwelling offshore

(Figure S3). In coordination with reduced subsurface DIC throughout the region, these changes in circulation contribute toward anomalous uptake of CO_2 throughout the CalCS. Note that the nearshore decomposition in Figure 7a has a y-axis range four times smaller than that of the offshore decomposition. This slight uptake anomaly is the result of a delicate balance of minor terms, where the sDIC reduction slightly outweighs the warming effect. On the other hand, the offshore region has contributions from SST and sDIC that are as much as triple the magnitude as that for the NPGO (Table 2). Despite the sDIC reduction being larger than the SST term, the reduced sAlk is substantial enough to cause a slight outgassing anomaly offshore (Figure 7b).

The direct response of winds to the NPGO and PDO plays a negligible role in influencing anomalous CO_2 flux in the CalCS (Table 2). Although ΔU in response to the NPGO and PDO is on the order of the HumCS and CanCS, $\frac{\partial F}{\partial U}$ is 3–10 times smaller than the other systems. $\frac{\partial F}{\partial U}$ is based on the climatological mean U, ΔpCO_2, and Schmidt number. The CalCS has the smallest mean ΔpCO_2 of the EBUS – just 0.2μatm. This causes CO_2 flux in the system to be relatively insensitive to fluctuations in the wind.

3.2.2 Humboldt Current

Global correlations between the HumCS CO_2 flux anomalies and SSTa display ENSO as a major ~~influencer~~influence, with regions of high correlation focused around the equatorial Pacific (Figure 5b). Correlations between HumCS CO_2 flux anomalies and the Nino3 index resulted in ~~an r-value~~ a correlation coefficient of -0.40 $\pm$ 0.04 (Figure 5e). Similar results were found for the Nino3.4 index (-0.38 $\pm$ 0.04) and the Nino4 index (-0.36 $\pm$ 0.05). We chose the Nino3 index as our primary predictor of HumCS CO_2 flux anomalies, since it is more eastern-focused and thus captures the stronger spatial correlations closest to the HumCS (Figure 5b).

We present the results of a linear Taylor expansion for HumCS CO_2 flux anomalies regressed onto a 1^{o}C El Niño in Figure 8 (~~Eq.~~ Equation 4). We find that the HumCS responds with a nearly single-signed CO_2 uptake anomaly, resulting in a weakening of the climatological outgassing (Figure 8b). Although there is a small region in the northern HumCS that responds with an outgassing anomaly, it ~~is nowhere near~~ not nearly as coherent across the ensemble as was the spatial dipole response of the CalCS to the PDO (Figure 7c). The direct regression of ΔF onto the Nino3 index results in an anomalous uptake of 0.49 mol m^{-2} yr^{-1} K^{-1}, which is approximately 18% of the long-term historical CO_2 flux mean of 2.8 mol m^{-2} yr^{-1}. As in the case of the CalCS, the two major terms contributing to the uptake anomaly are sDIC and SST, which are ~~in opposition to one another~~ of opposite sign (Figure 8a). We would anticipate this to be the case, as an El Niño event induces warming along the HumCS as well as reduces the efficacy of upwelling for bringing carbon- and nutrient-rich waters to the surface due to the presence of an anomalously deep thermocline (Figure S4; Strub et al., 1998). While upwelling-favorable winds tend to decrease along Chile (outside of our study region) during an El Niño event, the coastal wind response along Peru is variable, ranging anywhere from slight downwelling-favorable to slight upwelling-favorable anomalies (Wyrtki, 1975; Enfield, 1981; Huyer et al., 1987).

In CESM-LENS, the HumCS experiences a warming of 0.7^{o}C for a 1^{o}C El Niño, which results in an outgassing tendency of 0.3 mol m^{-2} yr^{-1} K^{-1} (Table 2). However, sDIC in the system is reduced by 13.2 mmol m^{-3} K^{-1} for the same event, which translates to a large uptake contribution of 0.8 mol m^{-2} yr^{-1} K^{-1} (Table 2). This is an enormous change in sDIC,

which is partially driven by the high subsurface DIC bias in the east equatorial Pacific in CESM1 (see Lovenduski et al., 2015, their Figure 2). The large sDIC reduction is due to weakened upwelling and a deepening of the thermocline by ~~advected warm waters~~ warm water advected from the equatorial Pacific (Figure S4). Although the passage of coastally trapped waves are important in the HumCS, they are not resolved in the coarse resolution CESM-LENS. Lastly, there is a minor outgassing anomaly of 0.06 mol m^{-2} yr^{-1} K^{-1} in response to a slight ~~intensification of wind magnitude~~ increase in wind speed during El Niño (Table 2). Despite the significant contributions of wind speed, SST, and sAlk toward outgassing, the large reduction in sDIC drives an uptake anomaly that weakens the HumCS outgassing during an El Niño event. Note that these are the same mechanisms that are responsible for reduced outgassing in the tropical belt in response to an El Niño (Feely et al., 1999).

3.2.3 Canary Current

Correlations between the CanCS CO_2 flux anomalies and SLPa globally reveal a region of high positive ~~r-values~~ correlation coefficients just northwest of Africa. This ~~encircles~~ coincides with the climatological position of the Azores High, the ~~atmospheric subtropical gyre~~ large-scale anticyclone which forces the CanCS. The climate index that most directly captures variability in the Azores High is the NAO, and will thus be considered the main mode of climate variability that modulates anomalous CO_2 flux in the CanCS. We find modest correlations of 0.28 ± 0.03 between annually smoothed CanCS CO_2 flux anomalies and the NAO (Figure 5f). Relatively lower correlations are expected between anomalous EBUS CO_2 fluxes and atmospheric indices, as the atmosphere is noisier than the more slowly evolving ocean.

Grid cell correlations between CanCS CO_2 flux anomalies and the NAO are displayed in Figure 9b. The CanCS has a nearly single-signed response of increased outgassing during the positive phase of the NAO. The direct regression of ΔF onto a 1σ NAO results in an outgassing anomaly of 0.2 mol m^{-2} yr^{-1} σ^{-1} (Table 2), which is 21% of the historical CO_2 flux mean of 0.95 mol m^{-2} yr^{-1}. ~~Also note that the linear Taylor approximation aligns exactly with the direct regression.~~ As with the other EBUS, the major contributors toward this anomaly are sDIC and SST (Figure 9a). The NAO ~~describes modifications to~~ represents fluctuations in the intensity of atmospheric ~~gyre~~ circulation between the Azores High and Icelandic Low (Hurrell et al., 2001). During the positive phase of the NAO, a stronger Azores High leads to intensified alongshore winds and thus more vigorous upwelling (Figure S5). This brings up additional deep cold water which in turn increases the CO_2 solubility of the system, tending toward an uptake anomaly of 0.15 mol m^{-2} yr^{-1} σ^{-1} (Table 2). On the other hand, the increased sDIC from intensified upwelling is double the magnitude of the SST contribution, despite the increased biological activity which reduces some of the physical sDIC input, leading to an outgassing anomaly of 0.33 mol m^{-2} yr^{-1} σ^{-1}. This large sDIC response is driven both by a high $\Delta sDIC$ of 3.9 mmol m^{-3}~~per 1σ NAO~~ σ^{-1} as well as the fact that the CanCS has the highest $\frac{\partial F}{\partial sDIC}$ of the major EBUS. Increased winds of 0.3 m s^{-1}~~per 1σ NAO~~ σ^{-1} lead to a significant outgassing pressure of 0.05 mol m^{-2} yr^{-1} σ^{-1}. This is due both to a large system sensitivity, $\frac{\partial F}{\partial U}$, to changes in wind and a high wind anomaly in response to the NAO. Ultimately, intensified winds and an anomalous increase in sDIC due to enhanced upwelling counteracts the solubility effects of colder SSTs and increased photosynthetic uptake of sDIC. ~~This leads to the highest relative CO_2 flux anomaly of any system, with a 21% increase in outgassing per 1σ NAO event relative to the long-term mean.~~

4 Discussion and Conclusions

We find that the seasonal cycle of pCO_2 is single-peaked and its phase is driven by thermal (solubility) effects in the CalCS, CanCS, and BenCS, while non-thermal effects modulate its amplitude. The seasonal cycle of pCO_2 in the HumCS is dual-peaked and driven by an ~~interchanging importance between~~ alternating dominance of thermal and non-thermal ~~factors~~effects. Although CESM-LENS models the CalCS and HumCS pCO_2 seasonal cycle well, the CanCS seasonal cycle is damped and ~~the BenCS seasonal cycle entirely~~ both the CanCS and BenCS seasonal cycles are nearly 180 degrees out of phase ~~.~~(Figure 2).

Variations in sDIC and SST in response to large modes of climate variability exert the most influence on anomalous CO_2 fluxes in the CalCS, CanCS, and HumCS. Further, these terms always act in opposition to one another in the portions of variability associated with the climate indices explored in this study. Secondary to these terms are wind speed and sAlk. Although their contributions do not rival those of SST and sDIC in magnitude, they act to further reinforce anomalies or to tip the balance toward outgassing or uptake when ~~sDIC and SST are of~~ the SST and sDIC associated terms are of about equal magnitude. In all systems, salinity and freshwater fluxes have negligible contributions toward the total CO_2 flux anomaly.

CalCS and CanCS CO_2 flux anomalies are associated mainly with climate modes related to ~~the subtropical anticyclonic gyres~~large-scale anticyclones, with their mean states (uptake for the CalCS and outgassing for the CanCS) intensified during phases of enhanced gyre circulation in the NPGO and NAO, respectively. ~~On the other hand,~~ CO_2 flux anomalies in the HumCS are mostly driven by ENSO, due to its close proximity to the equatorial Pacific. We find that the HumCS has weakened outgassing during El Niño due to reduced upwelling and a deepening of the thermocline, which are similar mechanisms to the equatorial Pacific's response to El Niño (Feely et al., 1999). ~~The major EBUS are often lumped together in studies due to their similarities – they are all characterized by their presence on the eastern flank of subtropical gyres, their Ekman dynamics associated with this positioning which leads to coastal and curl-driven upwelling, their productive fisheries, and in the case of our study, their high variability in CO_2 fluxes. However, we show in this study that their position in terms of latitude and ocean basin as well as their coastal geometry leads to unique physical and biogeochemical responses to climate variability. In particular, despite variations in sDIC being a leading contributor to CO_2 flux anomalies, the drivers of these sDIC anomalies differ between EBUS.~~

Because sDIC anomalies are so critical to the EBUS response to internal climate variability, we further decomposed these anomalies into their absolute (Table 3) and relative (Figure 10) contributions from circulation (e.g., upwelling, advection, ~~diffusion~~mixing), biology (photosynthesis, respiration, and calcium carbonate formation and dissolution), and air-sea CO_2 fluxes. Changes in biological activity in the HumCS in response to ENSO contribute to nearly 50% (~~8.611~~8.61 TgC yr^{-1} K^{-1}) of the total sDIC tendency anomaly (Figure 10, Table 3). During an El Niño (La Niña) enhanced respiration (photosynthesis) pumps sDIC into (out of) the upper water column. While biology is the major contributor to sDIC tendency anomalies in the HumCS, circulation changes play a leading role in the CalCS. In response to the NPGO, circulation anomalies in the CalCS contribute ~~to~~ roughly 47% (~~1.467~~1.47 TgC yr^{-1} σ^{-1}) of the total sDIC tendency anomaly (Figure 10, Table 3). It is difficult to assess the relative contributions of J'_{circ} and J'_{bio} in the CanCS, as the large ensemble spread in J'_{bio} drives a highly uncertain

J'_{circ}, which is computed as the anomaly of the other three terms (Figure 10). In all three systems, CO_2 flux anomalies play an important role in modifying the sDIC tendency, with an ensemble mean relative contribution greater than 25% (Figure 10). Note, however, that significant (moderate) spatial variability exists for circulation and biology contributions in the HumCS (CanCS), while contributions are relatively uniform throughout the CalCS (Figure S7).

It is important to note that anthropogenic climate change will likely modify our findings over the coming decades in a number of ways. The long-term addition of anthropogenic carbon to the surface ocean causes EBUS to become greater sinks for CO_2. This trend shifts the mean state of the EBUS, causing historical outgassing sites (the HumCS, CanCS, and BenCS) to become intermittent net sinks of CO_2 under the influence of internal variability by the end of the historical period (Figure 4). Projecting to 2100 under RCP8.5 forcing, we find that the CanCS and BenCS become net sinks for CO_2 due to the anthropogenic trend, with mean ~~values~~ CO_2 uptake of -0.43 mol m^{-2} yr^{-1} and -0.04 mol m^{-2} yr^{-1} over 2016–2100, respectively. The addition of anthropogenic CO_2 into the surface ocean can also intensify the magnitude of the seasonal cycle of CO_2 flux. This is due to the increased concentration of CO_2 in the surface ocean as well as the reduction in the ocean's buffer capacity, which makes pCO_2 more sensitive to seasonal fluctuations in DIC and alkalinity (Landschützer et al., 2018, and references therein). This effect has been shown in observations (Landschützer et al., 2018) and is also projected in climate models (Kwiatkowski and Orr, 2018), but is only seen significantly in the CalCS and CanCS in CESM-LENS, with an approximate 37% and 30% increase in the CO_2 flux seasonal cycle over 2016–2100, respectively. Negligible changes to the seasonal cycle ~~occur in the~~ over the next century are projected for the HumCS and BenCS in CESM-LENS.

External forcing will also alter the dynamics of the EBUS (Bakun et al., 2015; García-Reyes et al., 2015), potentially inducing changes to alongshore winds (Narayan et al., 2010; Sydeman et al., 2014; Oerder et al., 2015; Rykaczewski et al., 2015; Wang et al., 2015) and upper ocean stratification (Di Lorenzo et al., 2005; Rykaczewski and Dunne, 2010; Oerder et al., 2015), which will in turn influence the rate and efficacy of upwelling. It is unlikely that changes to vertical transport will be detectable until mid-century, as the anthropogenic signal is obscured by internal variability (Brady et al., 2017). However, externally forced trends in stratification are likely to emerge much quicker (Henson et al., 2016). The biogeochemical signature of waters feeding upwelling (e.g., O_2, CO_2, and nutrient concentrations) will likely also be modified due to these dynamical changes as well as to changes to ocean ventilation and source water pathways (Rykaczewski and Dunne, 2010). Externally forced changes in physical and biogeochemical properties of EBUS will likely alter the relative contributions of ~~variables~~ different physical processes to anomalous CO_2 fluxes, as approximated by Equation 4 and shown in Figures 6–9 and Table 2. It is also possible that modes of climate variability will change in response to anthropogenic forcing. Model projections and long-term observations have suggested that the intensity, frequency, or variance associated with ENSO (e.g., Timmermann et al., 1999; Cai et al., 2014, 2015), the NAO (Kuzmina et al., 2005), and the NPGO (Sydeman et al., 2013) has changed significantly in recent decades or will change over the next century. ~~While not observed in our historical modeling study,~~ These modifications to modes of climate variability ~~associated with the major EBUS could directly influence the magnitude of internally generated anomalies in~~ suggested by the literature could directly impact the response of EBUS CO_2 ~~fluxes in the future~~flux anomalies to internal variability, thus affecting the conclusions of our study. Further investigation of the impacts of anthropogenic climate change on CO_2 fluxes in EBUS is necessary for the community.

This study serves as a starting point toward better understanding how internal climate variability modulates CO_2 fluxes in the major EBUS. ~~Here, we only present the leading~~ We present the mode of climate variability ~~associated with~~ that has the largest influence on anomalous CO_2 fluxes in the HumCS and CanCS, and the leading two modes for the CalCS. Because of this, we ~~explain~~ account for approximately 16% of the total CO_2 flux variance in the HumCS and 8% in the CanCS. Since we analyzed statistically orthogonal modes (the PDO and NPGO) in the CalCS, we ~~were able to explain~~ account for as much as 31% of the total CO_2 flux variance. It is difficult to explain a large chunk of the remaining variance for the EBUS, as other modes of internal variability are physically dependent on one another. Further, locally generated atmospheric noise in the EBUS can contribute substantially to the total modeled CO_2 flux variance. Previous studies that relate anomalous CO_2 fluxes to internal climate variability have explained similar amounts of variance. For example, Lovenduski et al. (2007) explains anywhere from 2% to 31% of CO_2 flux variance in the Southern Ocean in response to the Southern Annular Mode (SAM), McKinley et al. (2006) from 6% to 38% in the North Pacific in response to the PDO, and Gruber et al. (2002) 15% in the North Atlantic in response to the NAO.

Our study is limited by our use of a ~~coarse single~~ single coarse-resolution model ensemble, which carries uncertainty due to structural biases in the representation of the climate system and biogeochemistry, the ensemble's ability to accurately simulate the magnitude and frequency of internal climate variability, and processes that occur at a finer scale than the grid resolution. The community would benefit from future studies involving multiple single-model ensembles, which would reduce uncertainty due to structural biases, such as in the dynamics of the BenCS and the elevated sub-surface DIC concentration in the east equatorial Pacific in CESM-LENS. Due to model resolution, we do not ~~directly~~ resolve the coastal upwelling ~~process which~~ that induces vigorous outgassing within the first ~~O(10km)~~ ~50km of the coastline, such as in high-resolution model solutions by Turi et al. (2014) and Fiechter et al. (2014). This problem could be mitigated by nesting high-resolution EBUS simulations within a coarser global ensemble or by using regional mesh refinement techniques. This would allow the remote propagation of climate variability into the EBUS, while avoiding the high computational cost of running multiple high-resolution global simulations. In particular, the BenCS requires significant attention. We find pronounced internal variability in CO_2 fluxes in the BenCS in CESM-LENS that warrants investigation in a high-resolution model specific to the BenCS. We anticipate that these results and further investigation of the relationship between internal climate variability and anomalous CO_2 fluxes in EBUS will be useful for the rapidly developing subseasonal to decadal prediction community. Skillful prediction of climate variability, such as ENSO, the NPGO, and NAO, could be linked directly to anomalous fluxes of CO_2 in the major EBUS. As these systems are naturally sensitive to the undersaturation of calcium carbonate, these predictions could also aid in detecting and managing the onset of seasonal ocean acidification.

Data availability. The output from CESM-LENS is available as single variable time series at monthly, daily, and 6-hourly resolution through the Earth System Grid. Instructions for access and a full listing of available variables can be found under the UCAR Large Ensemble Project web page. Also on the CESM-LENS project page is the Climate Variability Diagnostics Package (CVDP), which includes the climate indices

used in this study for every simulation. Instructions for accessing the NPGO index for each simulation as well the code used to generate it can be found at http://www.cesm.ucar.edu/projects/community-projects/LENS/projects/npgo.html.

Author contributions. RXB and NSL designed the study. RXB analyzed the data, prepared figures and tables, and wrote the paper. NSL, MAA, MJ, and NG provided invaluable feedback throughout the study and reviewed the paper.

Competing interests. The authors of this study are unaware of any conflict of interest.

Acknowledgements. The National Science Foundation sponsors the National Center for Atmospheric Research where the Community Earth System Model is developed. Computing resources were provided by NCAR's Computational and Information Systems Laboratory. The Department of Energy's Computational Science Graduate Fellowship supported RXB throughout this study (DE-FG02-97ER25308). NSL and RXB are grateful for support from NSF (OCE-1752724, OCE-1558225). NG is grateful for support from the SNF project CALNEX (grant no.149384) and ETH Zürich. We thank A. Phillips for his extensive work on developing the Climate Variability Diagnostics Package. We are grateful to two anonymous reviewers for their suggestions which helped in improving this manuscript. K. Karnauskas, J. Small, and M. Long provided feedback on earlier versions of this manuscript.

References

D. C. E. Bakker, B. Pfeil, K. M. O'Brien, K. I. Currie, S. D. Jones, C. S. Landa, S. K. Lauvset, N. Metzl, D. R. Munro, S.-I. Nakaoka, A. Olsen, D. Pierrot, S. Saito, K. Smith, C. Sweeney, T. Takahashi, C. Wada, R. Wanninkhof, S. R. Alin, M. Becker, R. G. J. Bellerby, A. V. Borges, J. Boutin, Y. Bozec, E. Burger, W.-J. Cai, R. D. Castle, C. E. Cosca, M. D. DeGrandpre, M. Donnelly, G. Eischeid, R. A. Feely, T. Gkritzalis, M. González-Dávila, C. Goyet, A. Guillot, N. J. Hardman-Mountford, J. Hauck, M. Hoppema, M. P. Humphreys, C. W. Hunt, J. S. P. Ibánhez, T. Ichikawa, M. Ishii, L. W. Juranek, V. Kitidis, A. Körtzinger, U. K. Koffi, A. Kozyr, A. Kuwata, N. Lefèvre, C. Lo Monaco, A. Manke, P. Marrec, J. T. Mathis, F. J. Millero, N. Monacci, P. M. S. Monteiro, A. Murata, T. Newberger, Y. Nojiri, I. Nonaka, A. M. Omar, T. Ono, X. A. Padín, G. Rehder, A. Rutgersson, C. L. Sabine, J. Salisbury, J. M. Santana-Casiano, D. Sasano, U. Schuster, R. Sieger, I. Skjelvan, T. Steinhoff, K. Sullivan, S. C. Sutherland, A. Sutton, K. Tadokoro, M. Telszewski, H. Thomas, B. Tilbrook, S. van Heuven, D. Vandemark, D. W. Wallace, and R. Woosley. Surface Ocean CO2 Atlas (SOCAT) V4, 2016.

A. Bakun, B. A. Black, S. J. Bograd, M. García-Reyes, A. J. Miller, R. R. Rykaczewski, and W. J. Sydeman. Anticipated effects of climate change on coastal upwelling ecosystems. *Current Climate Change Reports*, 1(2):85–93, Jun 2015. ISSN 2198-6061. https://doi.org/10.1007/s40641-015-0008-4.

R. T. Barber and F. P. Chavez. Biological consequences of El Niño. *Science*, 222(4629):1203–1210, 1983. ISSN 0036-8075. https://doi.org/10.1126/science.222.4629.1203.

R. T. Barber and F. P. Chávez. Ocean variability in relation to living resources during the 1982–83 El Niño. *Nature*, 319:279 EP –, 01 1986.

A. V. Borges and M. Frankignoulle. Distribution of surface carbon dioxide and air-sea exchange in the upwelling system off the galician coast. *Global Biogeochemical Cycles*, 16(2), 2002.

M. F. Borges, A. M. P. Santos, N. Crato, H. Mendes, and B. Mota. Sardine regime shifts off Portugal: a time series analysis of catches and wind conditions. *Scientia Marina*, 67(S1):235–244, Apr. 2003. ISSN 1886-8134, 0214-8358. https://doi.org/10.3989/scimar.2003.67s1235.

A. Boyd, J. Salat, and M. Masó. The seasonal intrusion of relatively saline water on the shelf off northern and central Namibia. *South African Journal of Marine Science*, 5(1):107–120, 1987.

R. X. Brady, M. A. Alexander, N. S. Lovenduski, and R. R. Rykaczewski. Emergent anthropogenic trends in California Current upwelling. *Geophysical Research Letters*, 44(10):5044–5052, 2017.

C. S. Bretherton, M. Widmann, V. P. Dymnikov, J. M. Wallace, and I. Bladé. The effective number of spatial degrees of freedom of a time-varying field. *Journal of Climate*, 12(7):1990–2009, 1999. https://doi.org/10.1175/1520-0442(1999)012<1990:TENOSD>2.0.CO;2.

W. Cai, S. Borlace, M. Lengaigne, P. Van Rensch, M. Collins, G. Vecchi, A. Timmermann, A. Santoso, M. J. McPhaden, L. Wu, et al. Increasing frequency of extreme El Niño events due to greenhouse warming. *Nature climate change*, 4(2):111, 2014.

W. Cai, G. Wang, A. Santoso, M. J. McPhaden, L. Wu, F.-F. Jin, A. Timmermann, M. Collins, G. Vecchi, M. Lengaigne, et al. Increased frequency of extreme La Niña events under greenhouse warming. *Nature Climate Change*, 5(2):132–137, 2015.

W.-J. Cai, M. Dai, and Y. Wang. Air-sea exchange of carbon dioxide in ocean margins: A province-based synthesis. *Geophysical Research Letters*, 33(12), 2006. https://doi.org/10.1029/2006GL026219.

Antonietta Capotondi, Andrew T Wittenberg, Matthew Newman, Emanuele Di Lorenzo, Jin-Yi Yu, Pascale Braconnot, Julia Cole, Boris Dewitte, Benjamin Giese, Eric Guilyardi, et al. Understanding ENSO diversity. *Bulletin of the American Meteorological Society*, 96(6): 921–938, 2015.

F. Chan, J. A. Barth, C. A. Blanchette, R. H. Byrne, F. Chavez, O. Cheriton, R. A. Feely, G. Friederich, B. Gaylord, T. Gouhier, S. Hacker, T. Hill, G. Hofmann, M. A. McManus, B. A. Menge, K. J. Nielsen, A. Russell, E. Sanford, J. Sevadjian, and L. Wash-

burn. Persistent spatial structuring of coastal ocean acidification in the California Current System. *Scientific Reports*, 7(1):2526, 2017. https://doi.org/10.1038/s41598-017-02777-y.

F. P. Chavez and M. Messié. A comparison of Eastern Boundary Upwelling Ecosystems. *Progress in Oceanography*, 83(1):80–96, 2009. https://doi.org/https://doi.org/10.1016/j.pocean.2009.07.032.

F. P. Chavez, J. T. Pennington, C. G. Castro, J. P. Ryan, R. P. Michisaki, B. Schlining, P. Walz, K. R. Buck, A. McFadyen, and C. A. Collins. Biological and chemical consequences of the 1997–1998 El Niño in central california waters. *Progress in Oceanography*, 54(1):205–232, 2002. https://doi.org/https://doi.org/10.1016/S0079-6611(02)00050-2.

FP Chavez, PG Strutton, GE Friederich, RA Feely, GC Feldman, DG Foley, and MJ McPhaden. Biological and chemical response of the equatorial Pacific Ocean to the 1997-98 El Niño. *Science*, 286(5447):2126–2131, 1999.

D. B. Chelton, P. A. Bernal, and J. A. McGowan. Large-scale interannual physical and biological interaction in the California Current. *Journal of Marine Research*, 40(4):1095–1125, 1982.

F. Chenillat, P. Rivière, X. Capet, E. Di Lorenzo, and B. Blanke. North Pacific Gyre Oscillation modulates seasonal timing and ecosystem functioning in the California Current upwelling system. *Geophysical Research Letters*, 39(1), 2012. https://doi.org/10.1029/2011GL049966.

K. Chhak and E. Di Lorenzo. Decadal variations in the California Current upwelling cells. *Geophysical Research Letters*, 34(14), 2007. https://doi.org/10.1029/2007GL030203.

F. Colas, X. Capet, J. McWilliams, and A. Shchepetkin. 1997–1998 El Niño off Peru: A numerical study. *Progress in Oceanography*, 79 (2-4):138–155, 2008.

T. E. Cropper, E. Hanna, and G. R. Bigg. Spatial and temporal seasonal trends in coastal upwelling off Northwest Africa, 1981–2012. *Deep Sea Research Part I: Oceanographic Research Papers*, 86:94–111, 2014. https://doi.org/https://doi.org/10.1016/j.dsr.2014.01.007.

M. D. DeGrandpre, T. R. Hammar, and C. D. Wirick. Short-term pCO2 and O2 dynamics in California coastal waters. *Deep Sea Research Part II: Topical Studies in Oceanography*, 45(8):1557–1575, 1998. https://doi.org/https://doi.org/10.1016/S0967-0645(98)80006-4.

C. Deser, I. R. Simpson, K. A. McKinnon, and A. S. Phillips. The Northern Hemisphere extratropical atmospheric circulation response to ENSO: How well do we know it and how do we evaluate models accordingly? *Journal of Climate*, 30(13):5059–5082, 2017.

C. Deser, I. R. Simpson, A. S. Phillips, and K. A. McKinnon. How well do we know ENSO's climate impacts over North America, and how do we evaluate models accordingly? *Journal of Climate*, 2018.

E. Di Lorenzo and N. Mantua. Multi-year persistence of the 2014/15 North Pacific marine heatwave. *Nature Climate Change*, 6(11): 1042–1047, 2016.

E. Di Lorenzo, A. J. Miller, N. Schneider, and J. C. McWilliams. The warming of the California Current System: Dynamics and ecosystem implications. *Journal of Physical Oceanography*, 35(3):336–362, 2005.

E. Di Lorenzo, N. Schneider, K. M. Cobb, P. J. S. Franks, K. Chhak, A. J. Miller, J. C. McWilliams, S. J. Bograd, H. Arango, E. Curchitser, T. M. Powell, and P. Rivière. North Pacific Gyre Oscillation links ocean climate and ecosystem change. *Geophysical Research Letters*, 35(8), 2008. https://doi.org/10.1029/2007GL032838.

E. Di Lorenzo, J. Fiechter, N. Schneider, A. Bracco, A. J. Miller, P. J. S. Franks, S. J. Bograd, A. M. Moore, A. C. Thomas, W. Crawford, A. Peña, and A. J. Hermann. Nutrient and salinity decadal variations in the central and eastern North Pacific. *Geophysical Research Letters*, 36(14), 2009. https://doi.org/10.1029/2009GL038261.

Emanuele Di Lorenzo and Mark D Ohman. A double-integration hypothesis to explain ocean ecosystem response to climate forcing. *Proceedings of the National Academy of Sciences*, 110(7):2496–2499, 2013.

D. Enfield. Thermally driven wind variability in the planetary boundary layer above Lima, Peru. *Journal of Geophysical Research: Oceans*, 86(C3):2005–2016, 1981.

R. Escribano, G. Daneri, L. Farías, V. A. Gallardo, H. E. González, D. Gutiérrez, C. B. Lange, C. E. Morales, O. Pizarro, O. Ulloa, and M. Braun. Biological and chemical consequences of the 1997–1998 El Niño in the Chilean coastal upwelling system: a synthesis. *Deep Sea Research Part II: Topical Studies in Oceanography*, 51(20):2389–2411, 2004. https://doi.org/https://doi.org/10.1016/j.dsr2.2004.08.011.

W. Evans, B. Hales, and P. G. Strutton. Seasonal cycle of surface ocean pCO2 on the Oregon shelf. *Journal of Geophysical Research: Oceans*, 116(C5), 2011. https://doi.org/10.1029/2010JC006625.

RA Feely, T Takahashi, R Wanninkhof, MJ McPhaden, CE Cosca, SC Sutherland, and Mary-Elena Carr. Decadal variability of the air-sea co2 fluxes in the equatorial pacific ocean. *Journal of Geophysical Research: Oceans*, 111(C8), 2006.

Richard A Feely, Rik Wanninkhof, Taro Takahashi, and Pieter Tans. Influence of El Niño on the equatorial Pacific contribution to atmospheric CO2 accumulation. *Nature*, 398(6728):597, 1999.

Jerome Fiechter, Enrique N Curchitser, Christopher A Edwards, Fei Chai, Nicole L Goebel, and Francisco P Chavez. Air-sea CO2 fluxes in the California Current: Impacts of model resolution and coastal topography. *Global Biogeochemical Cycles*, 28(4):371–385, 2014.

G. E. Friederich, P. M. Walz, M. G. Burczynski, and F. P. Chavez. Inorganic carbon in the central California upwelling system during the 1997–1999 El Niño–La Niña event. *Progress in Oceanography*, 54(1):185–203, 2002. https://doi.org/https://doi.org/10.1016/S0079-6611(02)00049-6.

M. Frischknecht, M. Münnich, and N. Gruber. Remote versus local influence of ENSO on the California Current System. *Journal of Geophysical Research: Oceans*, 120(2):1353–1374, 2015. https://doi.org/10.1002/2014JC010531.

M. Frischknecht, M. Münnich, and N. Gruber. Local atmospheric forcing driving an unexpected California Current System response during the 2015–2016 El Niño. *Geophysical Research Letters*, 44(1):304–311, 2017. https://doi.org/10.1002/2016GL071316.

M. García-Reyes, W. J. Sydeman, D. S. Schoeman, R. R. Rykaczewski, B. A. Black, A. J. Smit, and S. J. Bograd. Under pressure: Climate change, upwelling, and Eastern Boundary Upwelling Ecosystems. *Frontiers in Marine Science*, 2:109, 2015.

P. R. Gent, S. G. Yeager, R. B. Neale, S. Levis, and D. A. Bailey. Improvements in a half degree atmosphere/land version of the CCSM. *Climate Dynamics*, 34(6):819–833, 2010.

M. González-Dávila, J. M. Santana-Casiano, and I. R. Ucha. Seasonal variability of fCO2 in the Angola-Benguela region. *Progress in Oceanography*, 83(1-4):124–133, 2009.

L. Gregor and P. Monteiro. Is the southern Benguela a significant regional sink of CO2? *South African Journal of Science*, 109(5-6):01–05, 2013.

N. Gruber. Carbon at the coastal interface. *Nature; London*, 517(7533):148–149, Jan. 2015. ISSN 00280836.

N. Gruber, C. D. Keeling, and N. R. Bates. Interannual variability in the North Atlantic Ocean carbon sink. *Science*, 298(5602):2374–2378, 2002. ISSN 0036-8075. https://doi.org/10.1126/science.1077077.

B. Hales, T. Takahashi, and L. Bandstra. Atmospheric CO2 uptake by a coastal upwelling system. *Global Biogeochemical Cycles*, 19(1), 2005. https://doi.org/10.1029/2004GB002295.

J. Hauck. Unsteady seasons in the sea. *Nature Climate Change*, 8(2):97–98, 2018. https://doi.org/10.1038/s41558-018-0069-1.

C. Hauri, N. Gruber, G.-K. Plattner, S. Alin, R. A. Feely, B. Hales, and P. A. Wheeler. Ocean Acidification in the California Current System. *Oceanography*, 22(4):60–71, Dec. 2009.

Stephanie A Henson, Claudie Beaulieu, and Richard Lampitt. Observing climate change trends in ocean biogeochemistry: when and where. *Global change biology*, 22(4):1561–1571, 2016.

James W Hurrell, Yochanan Kushnir, and Martin Visbeck. The North Atlantic Oscillation. *Science*, 291(5504):603–605, 2001.

James W Hurrell, Marika M Holland, Peter R Gent, Steven Ghan, Jennifer E Kay, Paul J Kushner, J-F Lamarque, William G Large, D Lawrence, Keith Lindsay, et al. The Community Earth System Model: A framework for collaborative research. *Bulletin of the American Meteorological Society*, 94(9):1339–1360, 2013.

L Hutchings, CD Van der Lingen, LJ Shannon, RJM Crawford, HMS Verheye, CH Bartholomae, AK Van der Plas, D Louw, A Kreiner, M Ostrowski, et al. The Benguela Current: An ecosystem of four components. *Progress in Oceanography*, 83(1-4):15–32, 2009.

A. Huyer, R. L. Smith, and T. Paluszkiewicz. Coastal upwelling off Peru during normal and El Niño times, 1981–1984. *Journal of Geophysical Research: Oceans*, 92(C13):14297–14307, 1987.

M. G. Jacox, S. J. Bograd, E. L. Hazen, and J. Fiechter. Sensitivity of the California Current nutrient supply to wind, heat, and remote ocean forcing. *Geophysical Research Letters*, 42(14):5950–5957, 2015.

Jochen Kämpf and Piers Chapman. *Upwelling Systems of the World*. Springer, 2016.

J. E. Kay, C. Deser, A. Phillips, A. Mai, C. Hannay, G. Strand, J. M. Arblaster, S. C. Bates, G. Danabasoglu, J. Edwards, M. Holland, P. Kushner, J.-F. Lamarque, D. Lawrence, K. Lindsay, A. Middleton, E. Munoz, R. Neale, K. Oleson, L. Polvani, and M. Vertenstein. The Community Earth System Model (CESM) Large Ensemble Project: A community resource for studying climate change in the presence of internal climate variability. *Bulletin of the American Meteorological Society*, 96(8):1333–1349, 2015. https://doi.org/10.1175/BAMS-D-13-00255.1.

A. W. King, L. Dilling, G. P. Zimmerman, D. M. Fairman, R. A. Houghton, G. Marland, A. Z. Rose, and T. J. Wilbanks. *The first state of the carbon cycle report (SOCCR): The North American carbon budget and implications for the global carbon cycle.* U.S. Climate Change Science Program, Washington, 2007.

S. I. Kuzmina, L. Bengtsson, O. M. Johannessen, H. Drange, L. P. Bobylev, and M. W. Miles. The North Atlantic Oscillation and greenhouse-gas forcing. *Geophysical Research Letters*, 32(4), 2005.

L. Kwiatkowski and J. C. Orr. Diverging seasonal extremes for ocean acidification during the twenty-first century. *Nature Climate Change*, 8(2):141–145, 2018. https://doi.org/10.1038/s41558-017-0054-0.

P. Landschützer, N. Gruber, D. C. E. Bakker, U. Schuster, S. Nakaoka, M. R. Payne, T. P. Sasse, and J. Zeng. A neural network-based estimate of the seasonal to inter-annual variability of the Atlantic Ocean carbon sink. *Biogeosciences*, 10(11):7793–7815, Nov. 2013. ISSN 1726-4189. https://doi.org/10.5194/bg-10-7793-2013.

P Landschützer, N Gruber, DCE Bakker, and U Schuster. Recent variability of the global ocean carbon sink. *Global Biogeochemical Cycles*, 28(9):927–949, 2014.

P. Landschützer, N. Gruber, and D. C. E. Bakker. Decadal variations and trends of the global ocean carbon sink. *Global Biogeochemical Cycles*, 30(10):1396–1417, 2016. ISSN 1944-9224. https://doi.org/10.1002/2015GB005359.

P. Landschützer, N. Gruber, and D. C. E. Bakker. An updated observation-based global monthly gridded sea surface pCO2 and air-sea CO2 flux product from 1982 through 2015 and its monthly climatology (ncei accession 0160558). Version 2.2. NOAA National Centers for Environmental Information. Dataset., July 2017.

P. Landschützer, N. Gruber, D. C. E. Bakker, I. Stemmler, and K. D. Six. Strengthening seasonal marine CO2 variations due to increasing atmospheric CO2. *Nature Climate Change*, Jan. 2018. ISSN 1758-678X, 1758-6798. https://doi.org/10.1038/s41558-017-0057-x.

G. G. Laruelle, H. H. Dürr, C. P. Slomp, and A. V. Borges. Evaluation of sinks and sources of CO2 in the global coastal ocean using a spatially-explicit typology of estuaries and continental shelves. *Geophysical Research Letters*, 37(15), Aug. 2010. ISSN 00948276. https://doi.org/10.1029/2010GL043691.

G. G. Laruelle, R. Lauerwald, B. Pfeil, and P. Regnier. Regionalized global budget of the CO2 exchange at the air-water interface in continental shelf seas. *Global Biogeochem. Cycles*, 28(11):2014GB004832, Nov. 2014. ISSN 1944-9224. https://doi.org/10.1002/2014GB004832.

G. G. Laruelle, P. Landschützer, N. Gruber, J.-L. Tison, B. Delille, and P. Regnier. Global high-resolution monthly pCO2 climatology for the coastal ocean derived from neural network interpolation. *Biogeosciences*, 14(19):4545, 2017.

A. Leinweber, N. Gruber, H. Frenzel, G. E. Friederich, and F. P. Chavez. Diurnal carbon cycling in the surface ocean and lower atmosphere of Santa Monica Bay, California. *Geophysical Research Letters*, 36(8), Apr. 2009. ISSN 0094-8276. https://doi.org/10.1029/2008GL037018.

Keith Lindsay, Gordon B Bonan, Scott C Doney, Forrest M Hoffman, David M Lawrence, Matthew C Long, Natalie M Mahowald, J Keith Moore, James T Randerson, and Peter E Thornton. Preindustrial-control and twentieth-century carbon cycle experiments with the Earth System Model CESM1 (BGC). *Journal of Climate*, 27(24):8981–9005, 2014.

N. Lovenduski, M. Long, and K. Lindsay. Natural variability in the surface ocean carbonate ion concentration. *Biogeosciences*, 12(21): 6321–6335, 2015.

N. S. Lovenduski and N. Gruber. Impact of the Southern Annular Mode on Southern Ocean circulation and biology. *Geophys. Res. Lett.*, 32 (11):L11603, June 2005. ISSN 1944-8007. https://doi.org/10.1029/2005GL022727.

N. S. Lovenduski, N. Gruber, S. C. Doney, and I. D. Lima. Enhanced CO2 outgassing in the Southern Ocean from a positive phase of the Southern Annular Mode. *Global Biogeochem. Cycles*, 21(2), June 2007. ISSN 1944-9224. https://doi.org/10.1029/2006GB002900.

N. S. Lovenduski, G. A. McKinley, A. R. Fay, K. Lindsay, and M. C. Long. Partitioning uncertainty in ocean carbon uptake projections: Internal variability, emission scenario, and model structure. *Global Biogeochemical Cycles*, 30(9):1276–1287, 2016.

R. Lynn and S. Bograd. Dynamic evolution of the 1997–1999 El Niño–La Niña cycle in the southern California Current System. *Progress in Oceanography*, 54(1-4):59–75, July 2002. ISSN 00796611. https://doi.org/10.1016/S0079-6611(02)00043-5.

N. J. Mantua and S. R. Hare. The Pacific Decadal Oscillation. *Journal of oceanography*, 58(1):35–44, 2002.

N. J. Mantua, S. R. Hare, Y. Zhang, J. M. Wallace, and R. C. Francis. A Pacific Interdecadal Climate Oscillation with impacts on salmon production. *Bulletin of the American Meteorological Society*, 78(6):1069–1079, June 1997. ISSN 0003-0007. https://doi.org/10.1175/1520-0477(1997)078<1069:APICOW>2.0.CO;2.

G. A. McKinley, T. Takahashi, E. Buitenhuis, F. Chai, J. R. Christian, S. C. Doney, M.-S. Jiang, K. Lindsay, J. K. Moore, C. Le Quere, et al. North Pacific carbon cycle response to climate variability on seasonal to decadal timescales. *Journal of Geophysical Research: Oceans*, 111(C7), 2006.

R. Mogollón and P. H. Calil. On the effects of ENSO on ocean biogeochemistry in the Northern Humboldt Current System (NHCS): A modeling study. *Journal of Marine Systems*, 172:137–159, 2017.

I. Montes, W. Schneider, F. Colas, B. Blanke, and V. Echevin. Subsurface connections in the eastern tropical Pacific during La Niña 1999–2001 and El Niño 2002–2003. *Journal of Geophysical Research: Oceans*, 116(C12), 2011.

J Keith Moore, Keith Lindsay, Scott C Doney, Matthew C Long, and Kazuhiro Misumi. Marine ecosystem dynamics and biogeochemical cycling in the Community Earth System Model [CESM1 (BGC)]: Comparison of the 1990s with the 2090s under the RCP4. 5 and RCP8. 5 scenarios. *Journal of Climate*, 26(23):9291–9312, 2013.

N. Narayan, A. Paul, S. Mulitza, and M. Schulz. Trends in coastal upwelling intensity during the late 20th century. *Ocean Science*, 6(3):815, 2010.

V. Oerder, F. Colas, V. Echevin, F. Codron, J. Tam, and A. Belmadani. Peru-Chile upwelling dynamics under climate change. *Journal of Geophysical Research: Oceans*, 120(2):1152–1172, 2015.

Daniel Pauly and Villy Christensen. Primary production required to sustain global fisheries. *Nature*, 374(6519):255–257, 1995.

Adam S Phillips, Clara Deser, and John Fasullo. Evaluating modes of variability in climate models. *Eos, Transactions American Geophysical Union*, 95(49):453–455, 2014.

M. Pozo Buil and E. Di Lorenzo. Decadal dynamics and predictability of oxygen and subsurface tracers in the California Current System. *Geophysical Research Letters*, 44(9):4204–4213, 2017.

C. Reason, P. Florenchie, M. Rouault, and J. Veitch. Influences of large scale climate modes and Agulhas system variability on the BCLME region. In *Large Marine Ecosystems*, volume 14, pages 223–238. Elsevier, 2006. ISBN 978-0-444-52759-2. https://doi.org/10.1016/S1570-0461(06)80015-7.

R. R. Rykaczewski and J. P. Dunne. Enhanced nutrient supply to the California Current Ecosystem with global warming and increased stratification in an Earth System Model. *Geophysical Research Letters*, 37(21), 2010.

R. R. Rykaczewski, J. P. Dunne, W. J. Sydeman, M. García-Reyes, B. A. Black, and S. J. Bograd. Poleward displacement of coastal upwelling-favorable winds in the ocean's eastern boundary currents through the 21st century. *Geophysical Research Letters*, 42(15): 6424–6431, 2015.

J. H. Ryther. Photosynthesis and fish production in the sea. *Science*, 166(3901):72–76, 1969.

J. M. Santana-Casiano, M. González-Dávila, M.-J. Rueda, O. Llinás, and E.-F. González-Dávila. The interannual variability of oceanic CO2 parameters in the northeast Atlantic subtropical gyre at the ESTOC site. *Global Biogeochemical Cycles*, 21(1), 2007.

L. V. Shannon, A. J. Boyd, G. B. Brundrit, and J. Taunton-Clark. On the existence of an El Niño-type phenomenon in the Benguela System. *Journal of Marine Research*, 44(3):495–520, August 1986. https://doi.org/10.1357/002224086788403105.

R. J. Small, E. Curchitser, K. Hedstrom, B. Kauffman, and W. G. Large. The Benguela upwelling system: Quantifying the sensitivity to resolution and coastal wind representation in a global climate model. *Journal of Climate*, 28(23):9409–9432, 2015.

R Smith, P Jones, B Briegleb, F Bryan, G Danabasoglu, J Dennis, J Dukowicz, C Eden, B Fox-Kemper, P Gent, et al. The Parallel Ocean Program (POP) reference manual ocean component of the Community Climate System Model (CCSM) and Community Earth System Model (CESM). *Rep. LAUR-01853*, 141:1–140, 2010.

P. T. Strub, J. Mesias, V. Montecino, J. Rutllant, and S. Marchant. Coastal ocean circulation off western South America. In *The Sea*, volume 11. John Wiley, New York, 1998.

W. Sydeman, M. García-Reyes, D. Schoeman, R. Rykaczewski, S. Thompson, B. Black, and S. Bograd. Climate change and wind intensification in coastal upwelling ecosystems. *Science*, 345(6192):77–80, 2014.

W. J. Sydeman, J. A. Santora, S. A. Thompson, B. Marinovic, and E. D. Lorenzo. Increasing variance in North Pacific climate relates to unprecedented ecosystem variability off California. *Global Change Biology*, 19(6):1662–1675, 2013.

T. Takahashi, S. C. Sutherland, R. Wanninkhof, C. Sweeney, R. A. Feely, D. W. Chipman, B. Hales, G. Friederich, F. Chavez, C. Sabine, A. Watson, D. C. E. Bakker, U. Schuster, N. Metzl, H. Yoshikawa-Inoue, M. Ishii, T. Midorikawa, Y. Nojiri, A. Körtzinger, T. Steinhoff, M. Hoppema, J. Olafsson, T. S. Arnarson, B. Tilbrook, T. Johannessen, A. Olsen, R. Bellerby, C. S. Wong, B. Delille, N. R. Bates, and H. J. W. de Baar. Climatological mean and decadal change in surface ocean pCO2, and net sea–air CO2 flux over the global oceans. *Deep Sea Research Part II: Topical Studies in Oceanography*, 56(8):554–577, Apr. 2009. ISSN 0967-0645. https://doi.org/10.1016/j.dsr2.2008.12.009.

Taro Takahashi, Stewart C Sutherland, Richard A Feely, and Catherine E Cosca. Decadal variation of the surface water pco2 in the western and central equatorial pacific. *Science*, 302(5646):852–856, 2003.

Taro Takahashi, Stewart C. Sutherland, Colm Sweeney, Alain Poisson, Nicolas Metzl, Bronte Tilbrook, Nicolas Bates, Rik Wanninkhof, Richard A. Feely, Christopher Sabine, Jon Olafsson, and Yukihiro Nojiri. Global sea–air CO2 flux based on climatological surface ocean

pCO2, and seasonal biological and temperature effects. *Deep Sea Research Part II: Topical Studies in Oceanography*, 49(9):1601–1622, January 2002. ISSN 0967-0645. https://doi.org/10.1016/S0967-0645(02)00003-6.

D. W. J. Thompson, E. A. Barnes, C. Deser, W. E. Foust, and A. S. Phillips. Quantifying the role of internal climate variability in future climate trends. *Journal of Climate*, 28(16):6443–6456, 2015. https://doi.org/10.1175/JCLI-D-14-00830.1.

A. Timmermann, J. Oberhuber, A. Bacher, M. Esch, M. Latif, and E. Roeckner. Increased El Niño frequency in a climate model forced by future greenhouse warming. *Nature*, 398(6729):694, 1999.

Rodrigo Torres, David R Turner, José Rutllant, and Nathalie Lefèvre. Continued CO2 outgassing in an upwelling area off northern Chile during the development phase of El Niño 1997–1998 (July 1997). *Journal of Geophysical Research: Oceans*, 108(C10), 2003.

G. Turi, Z. Lachkar, and N. Gruber. Spatiotemporal variability and drivers of pCO2 and air–sea CO2 fluxes in the California Current System: an eddy-resolving modeling study. *Biogeosciences*, 11(3):671–690, Feb. 2014. ISSN 1726-4189. https://doi.org/10.5194/bg-11-671-2014.

Giuliana Turi, Zouhair Lachkar, Nicolas Gruber, and Martin Münnich. Climatic modulation of recent trends in ocean acidification in the California Current System. *Environmental Research Letters*, 11(1):014007, 2016.

G. Turi, M. A. Alexander, N. S. Lovenduski, A. Capotondi, J. D. Scott, C. A. Stock, J. P. Dunne, J. John, and M. G. Jacox. Response of O2 and pH to ENSO in the California Current System in a high resolution global climate model. *Ocean Sciences Discussion*, Aug. 2017.

D. Wang, T. C. Gouhier, B. A. Menge, and A. R. Ganguly. Intensification and spatial homogenization of coastal upwelling under climate change. *Nature*, 518(7539):390, 2015.

R. Wanninkhof. Relationship between wind speed and gas exchange over the ocean. *Journal of Geophysical Research: Oceans*, 97(C5): 7373–7382, 1992.

R. Wanninkhof. Relationship between wind speed and gas exchange over the ocean revisited: Gas exchange and wind speed over the ocean. *Limnology and Oceanography: Methods*, 12(6):351–362, June 2014. ISSN 15415856. https://doi.org/10.4319/lom.2014.12.351.

K. Wyrtki. El Niño—the dynamic response of the equatorial Pacific Ocean to atmospheric forcing. *Journal of Physical Oceanography*, 5(4): 572–584, 1975.

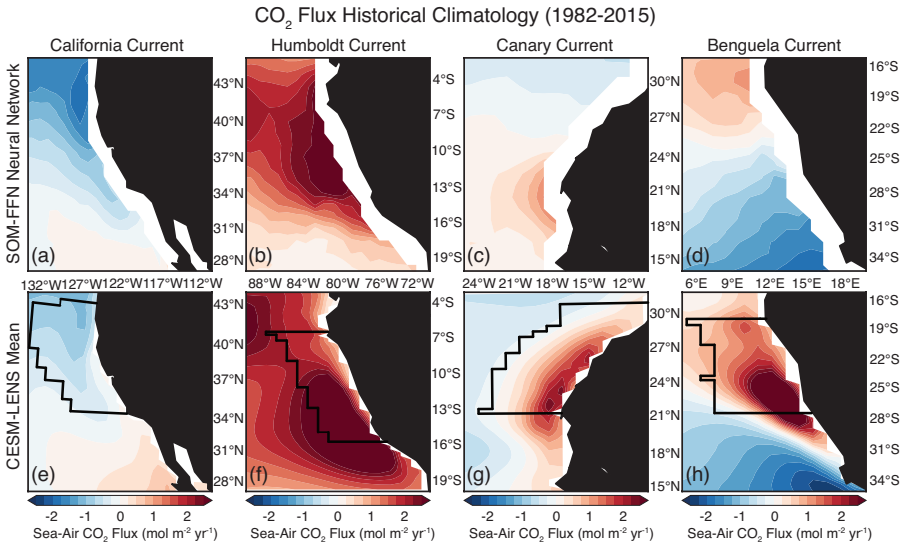

Figure 1. Comparison of CO_2 flux climatology from 1982–2015 between the SOM-FFN (a–d) and the CESM-LENS (e–h). Red denotes outgassing of CO_2 from the ocean to the atmosphere, while blue represents uptake of CO_2 by the ocean. Black lines in e–h follow the model grid and show the region used in each EBUS for statistical analysis, which is based on the 10^o latitude of most active upwelling from Chavez and Messié (2009) and confined to 800km offshore in the E–W direction.

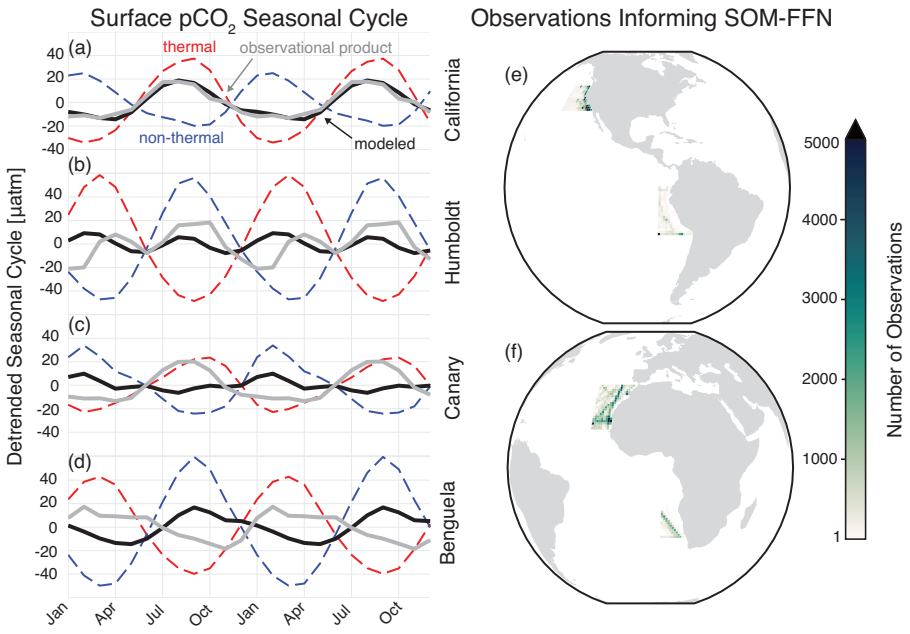

Figure 2. Detrended surface pCO_2 seasonal cycle from 1982–2015 for the SOM-FFN (gray) and the CESM-LENS ensemble mean (black) for the (a) CalCS, (b) HumCS, (c) CanCS, (d) and BenCS. Dashed red lines show the thermal component of the seasonal cycle for the CESM-LENS and dashed blue lines show the non-thermal component. The total number of observations from SOCATv4 contributing to the SOM-FFN for the EBUS is shown in (e) and (f).

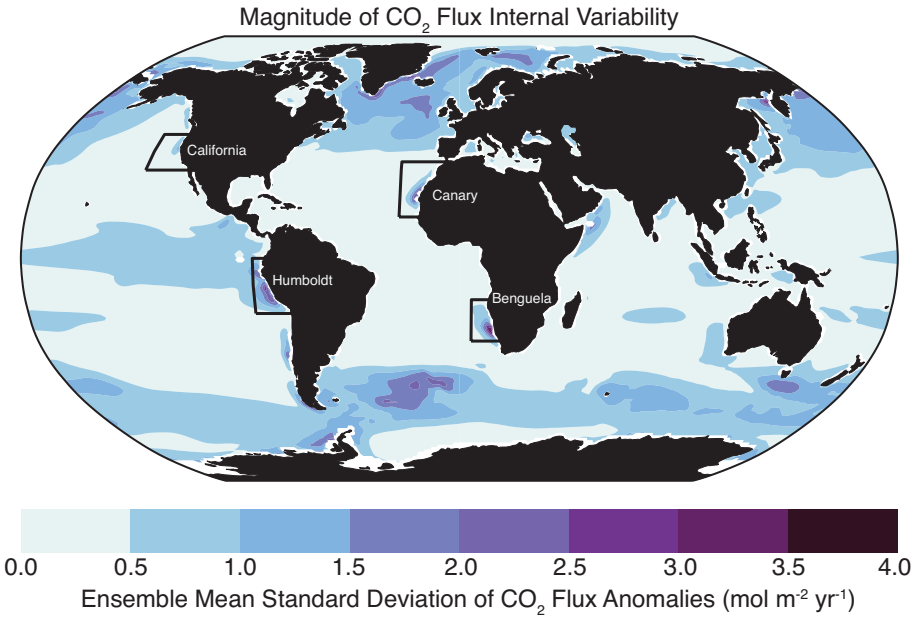

Figure 3. Magnitude of internal variability in CO_2 flux from 1920–2015 in the CESM-LENS. Anomalies were generated by removing the ensemble mean – which represents the seasonality and forced signal – from each realization. Internal variability was then quantified by taking the ensemble mean standard deviation of the anomalies from 1920–2015. Here, the black boxes outline the general domain of the EBUS in this study but do not coincide with the statistical boundaries shown in Figure 1.

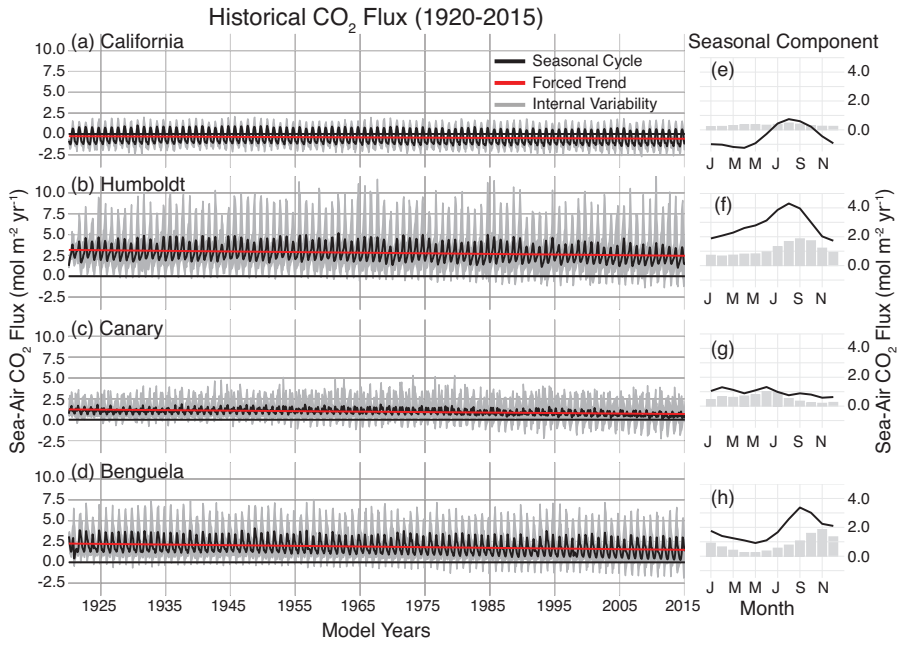

Figure 4. Time series of historical CO_2 flux (1920–2015) in the CESM-LENS for each of the four studied upwelling systems (a–d). The ensemble mean yields both the seasonal cycle (black) and the forced trend (red). Gray shading shows the bounds of the maximum and minimum realizations due to internal variability, but also contains signal from the seasonal cycle and forced trend. Table 1 displays the intercept, seasonality, internal variability, and forced trend for each system. Plots e–h show the mean seasonal cycle (black line) and ensemble mean monthly internal variability (gray bars) for 1920–2015 for each system.

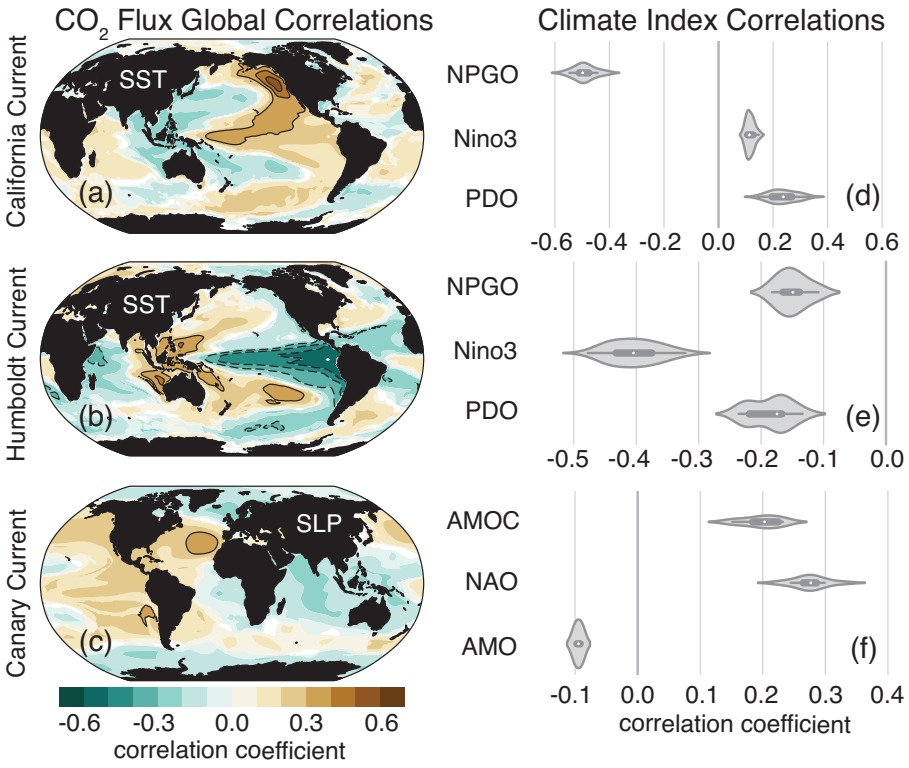

Figure 5. Correlations between area–weighted CO_2 flux anomalies in the statistical study regions outlined in black in Figure 1 (e–g) and SSTa (a–b; California, Humboldt) and SLPa (c; Canary) grid cells globally. Brown colors indicate that positive ~~values of~~ SSTa/SLPa ~~correlate~~ correlates with outgassing, and blue with uptake. Contour lines begin at $\pm$ 0.3 and progress in intervals of 0.1. Correlations were performed for each realization individually and the ensemble mean of those global correlations are presented here. Violin plots display correlations between area–weighted CO_2 flux anomalies from (a–c) with major modes of Pacific (d–e) and Atlantic (f) variability. The interior of the violin plot displays a box plot with the ensemble mean denoted as a white dot. Shading around the box plot reflects the ensemble distribution of correlations, which are mirrored on either side.

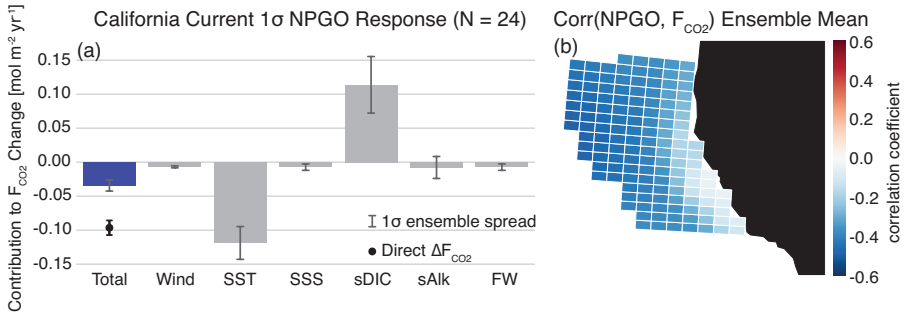

Figure 6. Linear Taylor expansion from ~~Eq.~~ Equation (4) for CalCS CO_2 flux anomalies regressed onto the NPGO (a). Gray bars represent the ensemble mean contributions of each variable to the CO_2 flux anomaly. Error bars represent the one standard deviation spread of the full ensemble. The individual bars sum to the "total" bar to approximate the direct regression of ΔF_{CO_2} onto the NPGO, which is denoted as the black dot with its associated ensemble spread. The ensemble mean grid cell correlations between CO_2 flux anomalies and the NPGO in the CalCS study region are displayed in (b). Positive correlations are associated with outgassing, negative with uptake. ~~Values~~ The magnitude and ensemble spread for each bar ~~are~~ is presented in Table 2.

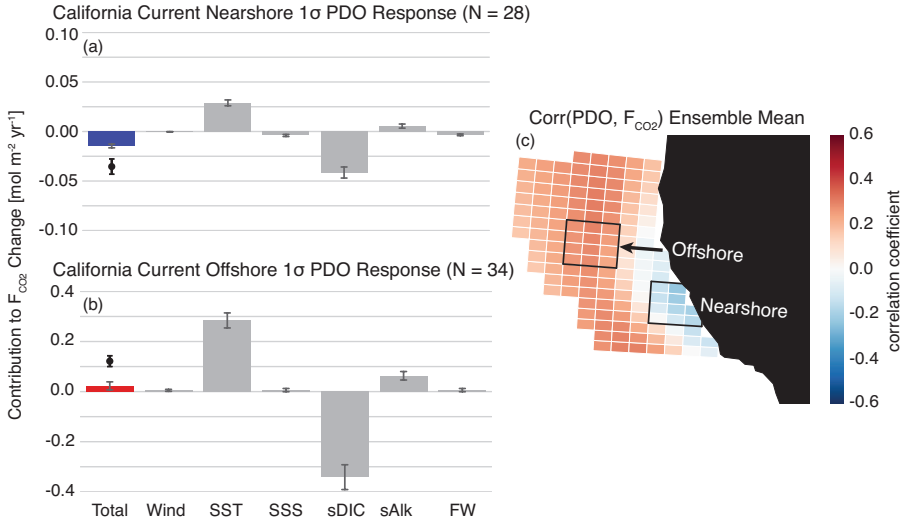

Figure 7. As in Figure 6, but in response to the PDO for a nearshore region (a) and offshore region (b). Note that the offshore decomposition (b) has a y-axis range four times that of the nearshore decomposition (a).

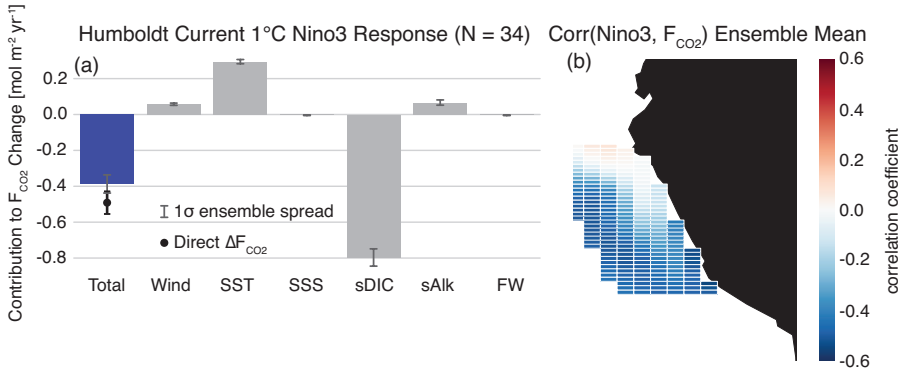

Figure 8. As in Figure 6, but for the Humboldt Current response to the Nino3 index.

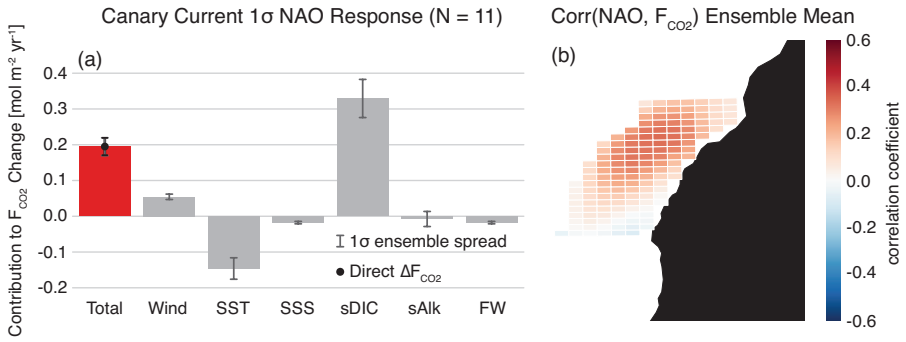

Figure 9. As in Figure 6, but for the Canary Current response to the NAO.

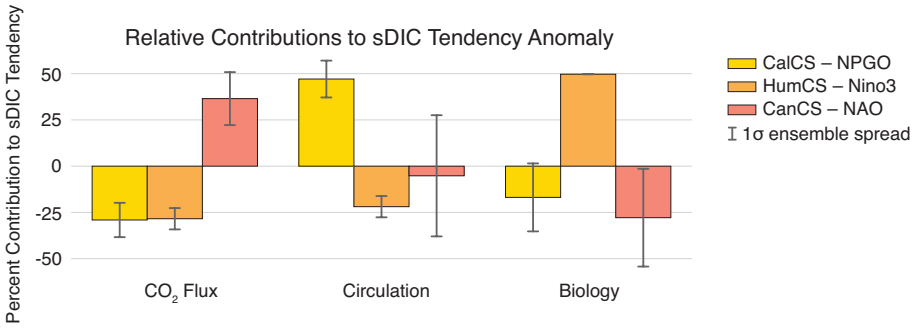

Figure 10. Relative contributions of anomalous air-sea CO_2 flux, physical circulation, and biology to the approximated sDIC tendency anomaly for the CalCS (yellow), HumCS (orange), and CanCS (red) in response to the NPGO, Nino3, and NAO, respectively. Error bars show the 1 standard deviation spread of the ensemble. For a given simulation, the absolute ~~values~~ magnitude of the three components sum to 100%. These values were approximated using Equation 5.

Table 1. Statistics for air-sea CO_2 fluxes in the CalCS, HumCS, CanCS, and BenCS from 1920–2015. The seasonal component is computed as the standard deviation of the ensemble monthly climatology after removing a fourth-order polynomial fit to remove the long-term trend. The internal component is computed as the ensemble mean standard deviation of the anomalies. The trend is computed as the first-order ordinary least squares regression coefficient for the contemporary (total), anthropogenic, and natural CO_2 fluxes. The intercept is derived from this linear regression. The non-seasonal component represents the fraction of total variability (seasonal plus internal) to which the internal component contributes.

Upwelling System	Intercept[1]	Seasonal[1]	Internal[1]	Trend (Contemporary)[2,3]	Trend (Anthropogenic)[2,3]	Trend (Natural)[2,3]	Non-Seasonal Component (%)
California (34^o N–44^o N)	-0.27	0.71	0.33	-0.31	-0.30	-0.01	31
Humboldt (16^o S–6^o S)	3.16	0.83	1.20	-0.71	-0.67	-0.04	59
Canary (21^o N–31^o N)	1.23	0.23	0.62	-0.56	-0.80	0.25	73
Benguela (28^o S–18^o S)	2.25	0.77	0.98	-0.76	-0.82	0.07	56

[1] mol m^{-2} yr^{-1}

[2] mol m^{-2} yr^{-1} $96yr^{-1}$

[3] All trends are significant to $\alpha = 0.05$ for a one-sided Mann-Kendall Test

Table 2. Estimated contributions of individual terms to air-sea CO_2 flux anomalies, ΔF, in response to a mode of climate variability using Equation 4. Each row under the *Individual Terms* header depicts the ensemble mean contribution and ensemble spread for Figures 6–9. The column "CalCS–PDOn" reflects results from the nearshore box in the CalCS in Figure 7, and "CalCS–PDOo" the offshore box. Σ is the sum of all contributing first-order terms (i.e., all rows under *Individual Terms* or the right hand side of Equation 4). ΔF is the direct regression of CO_2 flux anomalies onto the specified mode of climate variability (i.e., the left hand side of Equation 4).

Quantity	CalCS – NPGO[1]	CalCS – PDOo[1]	CalCS – PDOn[1]	HumCS – Nino3[2]	CanCS – NAO[1]
			Individual Terms		
$\frac{\partial F}{\partial U}\Delta U$	-0.01 $\pm$ 0.0	0.01 $\pm$ 0.0	0.0 $\pm$ 0.0	0.06 $\pm$ 0.01	0.05 $\pm$ 0.01
$\frac{\partial F}{\partial T}\Delta T$	-0.12 $\pm$ 0.02	0.28 $\pm$ 0.03	0.03 $\pm$ 0.0	0.29 $\pm$ 0.01	-0.15 $\pm$ 0.03
$\frac{\partial F}{\partial S}\Delta S$	-0.01 $\pm$ 0.0	0.01 $\pm$ 0.01	0.0 $\pm$ 0.0	-0.0 $\pm$ 0.0	-0.02 $\pm$ 0.0
$\frac{S}{S_0}\frac{\partial F}{\partial DIC}\Delta sDIC$	0.11 $\pm$ 0.04	-0.34 $\pm$ 0.05	-0.04 $\pm$ 0.01	-0.8 $\pm$ 0.05	0.33 $\pm$ 0.05
$\frac{S}{S_0}\frac{\partial F}{\partial Alk}\Delta sAlk$	-0.01 $\pm$ 0.02	0.06 $\pm$ 0.02	0.01 $\pm$ 0.0	0.07 $\pm$ 0.01	-0.01 $\pm$ 0.02
$\frac{\partial F}{\partial fw}\Delta fw$	-0.01 $\pm$ 0.0	0.01 $\pm$ 0.01	0.0 $\pm$ 0.0	0.0 $\pm$ 0.0	-0.02 $\pm$ 0.0
			Sum of Terms Versus Modeled		
Σ	-0.03 $\pm$ 0.01	0.02 $\pm$ 0.02	-0.01 $\pm$ 0.0	-0.38 $\pm$ 0.05	0.21 $\pm$ 0.03
~~ΔF_{mod}~~ ΔF	-0.10 $\pm$ 0.01	0.12 $\pm$ 0.02	-0.04 $\pm$ 0.01	-0.49 $\pm$ 0.06	0.2 $\pm$ 0.02

[1] mol m^{-2} yr^{-1} σ^{-1}
[2] mol m^{-2} yr^{-1} K^{-1}

Table 3. Regression coefficients between the given EBUS and climate index for anomaly time series of the estimated contributions toward the sDIC tendency integrated over the upper 100m and the total surface area of the system, as in Equation 5.[1]

Term	CalCS – NPGO[1]	HumCS – Nino3[2]	CanCS – NAO[1]
$\frac{dsDIC'}{dt}$	~~0.027~~ 0.03 ± ~~0.006~~ 0.01	~~-0.103~~ -0.10 ± ~~0.017~~ 0.02	~~0.044~~ 0.04 ± ~~0.009~~ 0.01
J'_{ex}	~~-0.762~~ -0.76 ± ~~0.195~~ 0.20	~~-4.840~~ -4.84 ± ~~0.613~~ 0.61	~~0.512~~ 0.51 ± ~~0.213~~ 0.21
J'_{bio}	~~-0.677~~ -0.68 ± ~~0.477~~ 0.48	~~8.611~~ 8.61 ± ~~0.813~~ 0.81	~~-0.491~~ -0.49 ± ~~0.543~~ 0.54
J'_{circ}	~~1.467~~ 1.47 ± ~~0.643~~ 0.64	~~-3.873~~ -3.87 ± ~~1.277~~ 1.28	~~0.023~~ 0.02 ± ~~0.552~~ 0.55

[1] TgC yr^{-1} σ^{-1}
[2] TgC yr^{-1} K^{-1}